Interpretation and analysis of the Blackfoot 3C-3D seismic survey

Grace Y.C. Yang, Don C. Lawton, Robert R. Stewart, Susan L. M. Miller, Collin C. Potter, and Vladan Simin

ABSTRACT

This paper describes the interpretation of the 3C-3D seismic survey acquired in Blackfoot field, near Strathmore, Alberta (Township 23, Range 23 W4).

Structural interpretation shows a horst block in the south-central part of the area, evident from basal Cambrian time through Viking time. A fault running in a north-south direction bounds the eastern part of the block at basal Cambrian time. The fault is clearly mappable on both *P-P* and *P-S* data. More detailed structural variations are noticed on the *P-S* time structure map than from *P-P* data in the west-central part of the survey area.

Time slice analysis indicates that P-P amplitude anomalies occur not only along the Glauconitic channel trend (target of survey), but also where regional wells were drilled. P-S time slices and isochron maps indicate clearly the valley fairway trend, and *Vp/Vs* values very accurately predict the locations of producing wells.

The Blackfoot 3C-3D survey has shown that converted-wave (P-S) analysis has provided significant added value to conventional, single-component P-wave surveys for the exploration of valley-fill sandstone reservoirs.

INTRODUCTION

The Blackfoot field is located in the southern Alberta, 45 km south-east from Calgary. The 3C-3D seismic survey was conducted by Boyd Exploration Consultants Ltd and the CREWES project in 1995. The objective was to evaluate the effectiveness of integrated *P-P* and *P-S* surveys for improved hydrocarbon exploration, primarily to demonstrate that 3C-3D seismic data can build on and improve conventional 3D *P* -wave data and provide additional stratigraphic and structural images of the subsurface, discriminate lithology, and test for anisotropy which may be caused by fracturing and regional stress directions (Lawton et al., 1995). The focus is to discriminate channel and regional seismic signatures, and to distinguish between sand-fill and shale-fill within the channel, e.g. to distinguish between porous sandstone and shale plug lithologies.

The interpretation of the Blackfoot 3C-3D seismic surveys presented in three parts: Firstly, examination of the geometric framework of the reservoir and the structure of the area; Secondly, *Vp/Vs* analysis; and thirdly, stratigraphic amplitude analysis of both *P-P* data and *P-S* wave data volumes.

GEOLOGICAL BACKGROUND

The reservoir in the Blackfoot field is producing from Glauconitic sand of the Lower Cretaceous Glauconitic Formation: It is a valley-fill depositional environment which has been well documented (Hopkins, 1987, & 1991; Strobl, 1988; Wood, 1989, 1992). In southern Alberta, the Glauconitic member is an unconformity bounded sequence that formed on an ancient coastal plain in response to relative sea level fluctuations (Wood, 1992). From well data in the Blackfoot area, it is interpreted that incised valley fill (or channel fill) sediments formed in an estuarine environment (Miller, et al., 1995). Figure 1 shows the stratigraphic sequence near the zone of interest (modified from Wood, 1992). The incised valley cuts to varying depths through the underlying strata and thus the base may be found directly overlying one of several formations.

Oil and gas are trapped stratigraphically within quartzose sandstones in incised valley or channels of the Glauconitic member in the Blackfoot area. Updip seals for these Glauconitic reservoirs are commonly pinch out of porous channel sands against impermeable sands or shales.

DATA SET

The 3C-3D seismic survey grid is shown in Figure 2. The vertical and radial component data were processed by two independent processing companies: Pulsonic Geophysical Ltd. and Sensor Geophysical Ltd. Since the data processed by Sensor covers only a portion of whole area, we will show the results of interpretation based primarily on data processed by Pulsonic. The quality of the data set is very good as shown in Figure 3 (*P-P* data) and 4 (*P-S* data). The zone of interest is at about 1050 ms on the *P-P* section and 1550 ms on the *P*-S section.

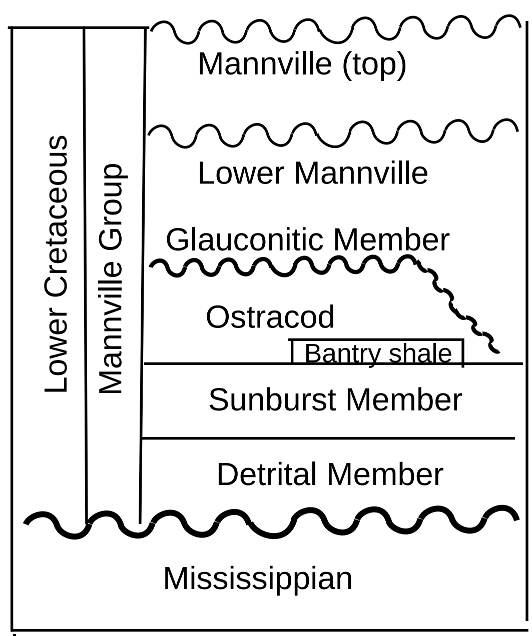

Fig. 1. Stratigraphic nomenclature of Cretaceous rocks in the Blackfoot area (modified from Hopkins, 1991)

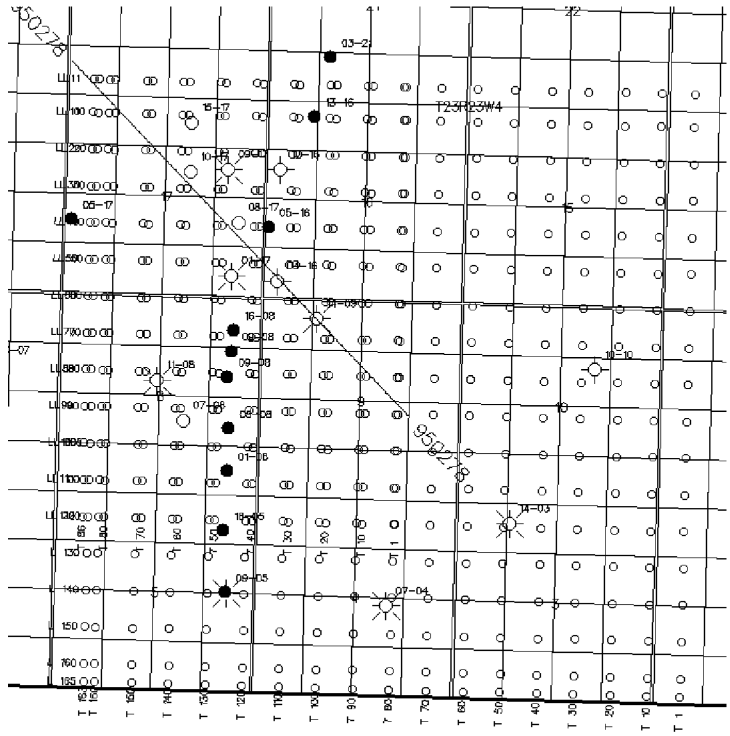

Fig. 2 Blackfoot 3C-3D seismic survey grid

ANALYSIS AND INTERPRETATION

A total of 18 wells were drilled in the area and sonic and density logs were available from 16 of these wells. Four wells have dipole logs with *P*- and *S*- sonic curves: 08-08, 09-17, 12-16, and 4-16. The 08-08 well has 38m of clean sand, 09-17 is a regional well which encountered Ostracod, and the 12-16 and 4-16 wells are shale plugged. VSP (Vertical Seismic Profiles) were recorded in two wells: 14-3 and 4-16; data quality was excellent, showing high-frequency content and correlation with the surface seismic data was straightforward. Well data were evaluated and tied the geological horizons with both *P-P* and *P-S* seismic data (details see chapter 37, this volume). Seven key seismic horizons (Viking, Mannville, Lower Mannville, Top Channel, Mississippian, Wabamun and basal Cambrian) were selected, interpreted and mapped because of their seismic continuity and adequate seismic-to-well correlation. They are identified and picked on both *P-P* and *P-S* sections. Examples of interpreted sections of both data components are shown in Figures 3 and 4. These seven key horizons form the framework for structural interpretation and isochron mapping.

For each horizon, a control grid of east-west inlines and north-south crosslines was defined using every 10th line, (every 300 m), for interpretation. Arbitrarily oriented lines were used to check and improve the consistency of the interpretation. The interactively interpreted control grid was then used as input to an automatic horizon picker using SeisX software (Photon Systems).

The interpretation proceeded by mapping Viking, Mannville, Lower Mannville, top channel, Mississippian, Wabamun and basal Cambrian events. Seismic amplitude variations across the zone of interest, i.e. near the top channel were evaluated, isochrons between these events were computed, and time slices were used to assist the interpretation.

Geometric framework and structure

The *P-P* time structure maps for each horizon are displayed in Figure 5a (basal Cambrian level), 6a (Wabamun event), 7a (Mississippian event), 8a (Top Channel event), 9a (Lower Mannville event), 10a (Mannville event), and 11a (Viking time). The *P-S* time structure maps of the same events are shown in Figures 5b, 6b, 7b, 8b, 9b, 10b, and 11b, respectively. The red/yellow color zones indicate lower traveltimes or structural highs, and delineate a horst block in the south-central part of the survey area. The horst block developed in pre-Wabamun times, but its influence on the time structure maps extends at least to Viking times (Lower Cretaceous). A fault running in a north-south direction bounds the eastern part of the block at basal Cambrian time (Figure 5a). It is clear on both *P-P* and *P-S* data. Note that more detailed structure variations are visible in the west-central area on *P-S* time structure maps (Figure 5b, 6b, etc.).

Time slice analysis

Time slice display and interpretation was undertaken by first flattening the data volume on a horizon above the Glauconitic channel level which could be picked confidently on both *P-P* and *P-S* data sets. The purpose was to remove long-wavelength structure from the data caused by drape and mid-Cretaceous uplift of the horst block in the center of the survey area. The Mannville event was chosen to flatten the volume on in this data set. In the absence of structure, time slices display stratigraphic or paleo-geomorphic features directly. The flattened volume permit stratigraphic and other depositional features to be recognized and studied in detail without confusion of structure.

Figure 12a is the time slice at 1054 ms from 3-D *P-P* volume. The time slice cuts the volume at about the level of the channel. The time slice in figure 12a shows an amplitude anomaly along the trend of oil wells (01-08 through 16-08) in the southern part of the Glauconitic patch. However, the channel signature is non-unique, with bright amplitudes also occurring at the locations of regional wells (14-09, 11-08). Figure 12b is the time slice section of *P-S* data volume at 1560 ms, which is equivalent to the level of the channel. The color bar represents the seismic reflection amplitude. The structure removal in flattening the Mannville showed a high-amplitude valley-like feature (the yellow/reds extend in the north-south direction across left central part of the image) across the survey area on the *P-S* data. Regional wells lie outside this interpreted channel trend. Figure 13a is a *P-P* time slice at 1080 ms, which is just above the Mississippian surface and possibly shows a Detrital channel. Figure 13b is the time slice of the *P-S* wave at same level. The reds/yellows and greens are seismic peaks (positive amplitude) and troughs (negative amplitude). The areas of color yellow have a weak seismic amplitude and the progressively darker reds indicate strengthening of the seismic amplitude. The greenish color running north-northeast to south on the left part of the image is also evident. It is significant that the *P-S* data appears to show the channel trend more vividly than does the *P-P* data.

The comparison of figure 12a with figure 13a (or figure 12b with figure 13b) suggests that the development of the Glauconitic channel locally in this area may associated with the paleo-topography at Mississippian time. It is also important to note that the elongate amplitude highs on the *P-S* time slice sections correlate to the well data better than the *P-P* time slices.

Isochron maps

Figure 14a is a *P-P* isochron map from the Mannville to Top Channel event, and Figure 14b is the equivalent map for *P-S* data. The *P-P* data (Fig. 14a) shows drape over the channel whereas the *P-S* data (Fig. 14b) shows an isochron thickening and no evidence of drape. It is interpreted that the Top Channel event on the *P-S* data has different tuning/interference effects than the *P-P* data has.

Figure 15a is the *P-P* isochron map of Wabamun to Lower Mannville and Figure 15b is the equivalent *P-S* isochron map. Note that there is a distinct thickness trend running north-south on the *P-P* isochron and also a thinning on the *P-S* isochron in the south-central part of the area, along the production wells. Both thickness on *P-P* isochron and thinning on *P-S* isochron are factors contributing to the lower *Vp/Vs* values along this trend, discussed in the next section.

Figures 16a and 16b are the isochron maps of Wabamun to Top Channel event from *P-P* and *P-S* respectively. Figures 17a and 17b are the isochron maps of Mississippian to Mannville event from *P-P* and *P-S* respectively. It is interesting to notice that the thickness on Figure 17b coincides with all the producing wells

V_p/V_s analysis

The *Vp/Vs* values across several horizon intervals were calculated using the relationship (Garotta, 1987):

$$Vp/Vs = 2\ t_{ps} / t_{pp} - 1$$

where t_{ps} is the *P-S* isochron and t_{pp} is the *P-P* isochron

Some results of the *Vp/Vs* analysis are shown in Figure 18a (Wabamun to Lower Mannville) and Figure 18b (Wabamun to Top Channel event). The red/yellow color indicates the value smaller than 1.87 on Figure 18a and lower than 1.84 in Figure 18b. The *Vp/Vs* values are expected to have a wider range of values for a thinner interval than the thicker interval; this is what we see from figures 18a and 18b. If *Vp/Vs* is beyond the expected range due to geological variations, it is an indication of mispicks, whereas reasonable values increase the confidence in the interpretation.

In Figures 18a and 18b, that 4-16 and 12-16 well positions lie within the zones of higher *Vp/Vs* (green/blue color zone), whereas the producing wells such as: 13-16, 5-16, 16-8, 102 / 9-8, 9-8, 8-8, 1-8 all lie in the zone of low *Vp/Vs* values (red / yellow color).

As to the lower target of Beaverhill Lake formation, the *Vp/Vs* distribution map from basal Cambrian to Wabamun event is shown in figure 18c. Generally there is a decrease in *Vp/Vs* along the margins of the horst block.

Stratigraphic Amplitude Analysis

Fig. 19a. 19b. 19c show the amplitude ratio of *P-S* data to *P-P* data on Top Channel event, Lower Mannville event, and Mississippian event respectively.

The amplitude of the seismic reflection can be altered by changes in caprock properties (density, velocity, and lithology); changes in reservoir properties (caused by change in porosity mineralogy, or fluid content); or changes in the geometry of the interface such as steep dips, faulting and fracturing. The lateral variations of these amplitude ratio of *P-S* and *P-P* data maps show that there may have some anisotropy presence in the survey area. The clear edge on Figure 19c (amplitude ratio of *P-S* and *P-P* data at Mississippian time) may be an indication of transition zone of sand to shale.

DISCUSSION AND CONCLUSION

Figure 20 is the interpreted distribution of Glauconitic channel sand bodies inferred from the time slices, the amplitude maps (Figures 19a, 19b, and 19c) and *Vp/Vs*. analysis (Figures 18a and 18b). In general, the Glauconitic channel sand bodies are concentrated in discrete bodies, and that only those sandstone bodies with favorable local structural disposition form reservoirs. The P-S data interpretation, particularly isochron analysis, shows the channel trend clearly, and *Vp/Vs* analysis show areas interpreted to be reservoir sands, which correlate spatially very well with the well control.

The interpretation of 3D-3D seismic data with well controls allows a structural and time stratigraphic reconstruction of lithofacies in the Blackfoot field. The techniques of mapping *Vp/Vs*, flattened time slices, and stratigraphic amplitude analysis has brought a new perspective to geophysical interpretation. The integration of both *P*- and *S*- wave data increases our ability to view the valley fairway and delineate spatial distribution of sand and shale in the area. We have also demonstrated that flattening to be a powerful method of separating structure from stratigraphy so that a depositional surface may be reconstituted, permitting depositional features, such as bars and channels to be followed in detail. We propose to further investigate the amplitude relationship between the *P-P* and *P-S* data.

REFERENCES

Brown, Alistair.R., 1979, 3-D seismic survey gives better data, Oil and Gas Journal , **77**, no. 45,. 57-71.

Brown, Alistair.R. and R.G. McBeath, 1980, 3-D seismic surveying for field development comes of age, Oil & Gas Journal, **78**, no. 46, 63-65.

Brown, Alistair R., Interpretation of three-dimensional seismic data, third edition, AAPG memoir **42**, American Association of Petroleum Geologists.

Brown, Alistair R., C.G. Dahm and R.J. Graebner, 1982, A stratigraphic case history using three-dimensional seismic data in the Gulf of Thailand, Geophys. Prosp. , **29**, 327-349.

Domenico, S. N. , 1984, Rock lithology an porosity determination from shear and compressional wave velocity: Geophysics, **49**, 1188 - 1195.

Garotta, R. , P. Marechal and M. Magesan, 1985, Two component acquisition as a routine procedure for recording P-waves and converted waves. J. of the Canadian Society of Exploration Geophysicists, **21**, no. 1, 40 - 53.

Hardage, Bob A. , R.A. Levey, V. Pendleton, J. Simmons, and R. Edwon, 1994, A 3-D seismic case history evaluating fluvially deposited thin-bed reservoirs in a gas-producing property, Geophysics, **59**, 11, 1650-1665.

Hautefeluille, A., and W.R. Cotton, 1979, Oil and Gas Journal, **77**,. no. 45,. 72-79.

Hopkins James M. et. at., 1991, Waterflood response of reservoirs in an estuarine valley fill: upper Mannville G, U, and W pools, Little Bow Field, Alberta, Canada: AAPG **75**, no. 6, 1064-1088.

Hopkins, John C., Lawton, Don C., and Gunn, Jack D., 1987, Geological and seismic evaluation of a Lower Mannville valley system: Alderson Prospect, Rolling Hills, southeastern Alberta: Bulletin of Canadian Petroleum Geology, **35**, 296-315.

Ikwuakor, K. C. , 1988, V_p / V_s revisited: pitfalls and new interpretation techniques, World Oil, September, 1988, 41 - 46.

Lawton, Don C, Robert R. Stewart, Andreas Cordsen, and Stacey Hrycak, 1995, Advances in 3C-3D design for converted waves: CREWES project Research Report, v. 7, 43. 1 - 43.41.

Miller, Susan L. M. Aydemir, M. E. and G.F. Margrave, 1995, Preliminary interpretation of P-P and P-S seismic data from the Blackfoot broad-band survey: CREWES project Research Report, v. 7, 42. 1 - 42.18.

Rosenthal, Lorne, 1988, Wave dominated shorelines and incised channel trends: Lower Cretaceous Glauconite formation, West-Central Alberta, , Sequences, Stratigraphy, sedimentology: surface and subsurface. Canadian Society of Petroleum Geologists, Memoir **15**, 207-220.

Strobl R. S., 1988, The effects of sea-level fluctuations on prograding shorelines and estuarine valley-fill sequences in the Glauconitic Member, Medicine River Field and adjacent areas, Canadian Soc. of Petroleum Geol. Memoir **15**, Sequences, Stratigraphy, Sedimentology: Surface and Subsurface. 221-236.

Tatham, R. H. , 1982, V_P / V_S and lithology: Geophysics, **47**, 336 - 344.

Tatham, R. H. , and P.L. Stoffa, 1976, V_P / V_S - A potential hydrocarbon indicator: Geophysics, **41**, 895 - 921.

Tatham, R. H. and M. D. McCormack, 1991, Multicomponent Seismology in Petroleum Exploration. Investigations in Geophysics Series Vol. 6. Society of Exploration Geophysics.

Tegland, E.R., 1977, 3-D seismic techniques boost field development, Oil and Gas Journal , **75**, no. 37, 79-82.

Wood, James M. and John C. Hopkins, 1989, Reservoir sandstone bodies in estuarine valley fill: Lower Cretaceous Glauconitic Member, Little Bow Field, Alberta, Canada, AAPG Bulletin, . **73**, no. 11, 1361-1382.

Wood, James M. and John C. Hopkins, 1992, Traps associated with paleovalleys and interfluves in an unconformity bounded sequence: Lower Cretaceous Glauconitic Member, southern Alberta, Canada: AAPG Bulletin **76**, 904-926.

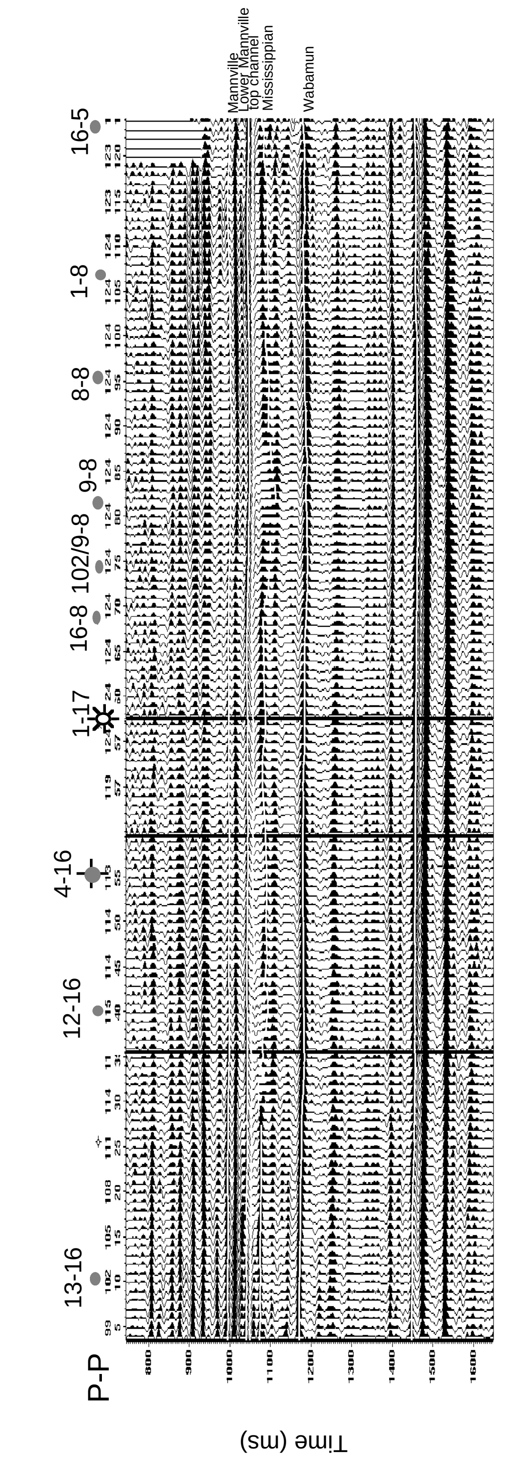

Fig. 3. An arbitrary N-S seismic line across most of the wells in the area

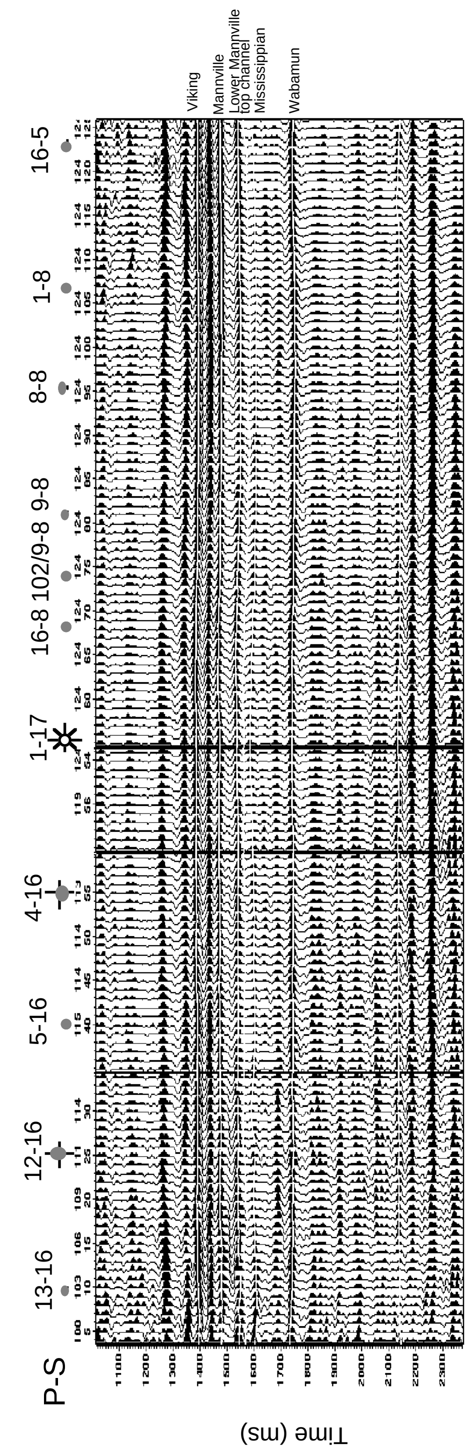

Fig. 4. P-S seismic line across same wells as in Figure 3

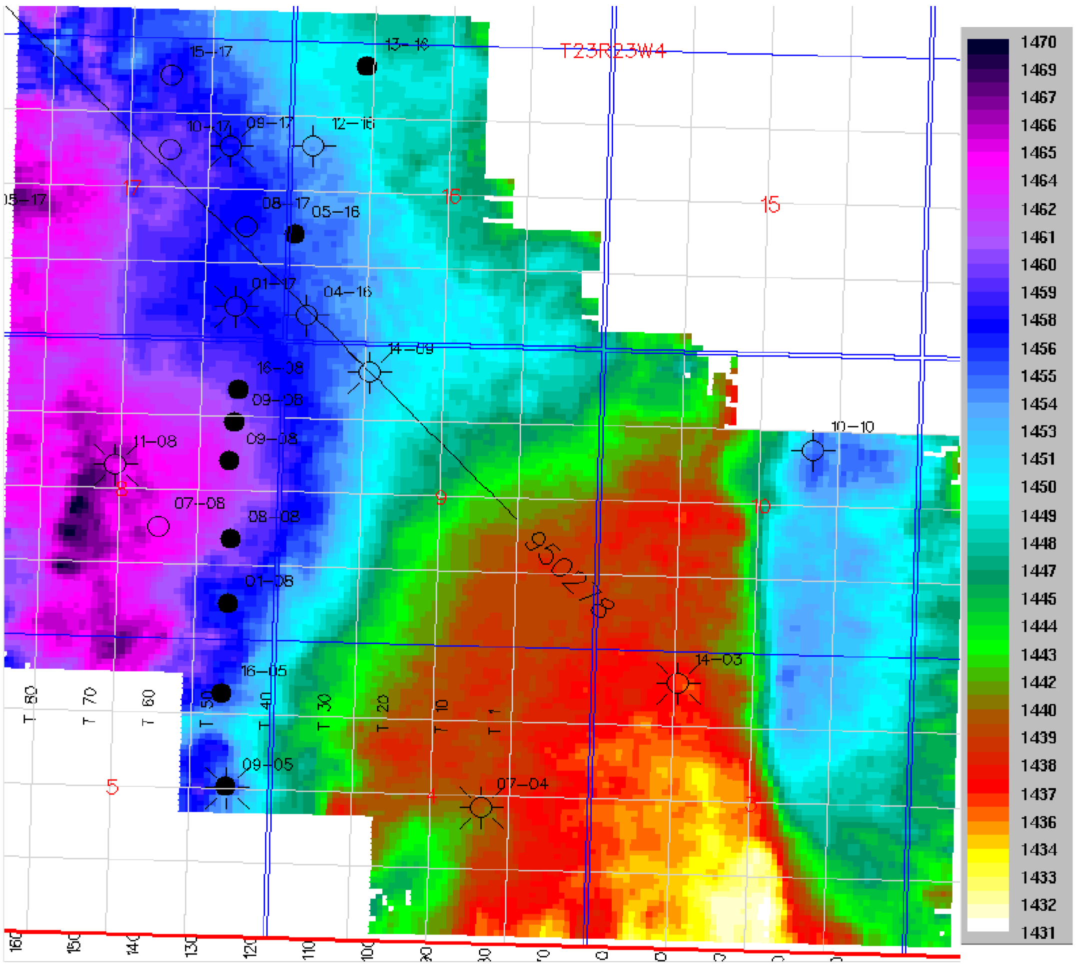

Fig. 5a. *P-P* time structure map, basal Cambrian event. The red/yellow color zones indicate the lower traveltimes or strucural highs, and delineate a horst block (width greater than a mile) in the south-central part of the area. This structure map shows the dip down to west, and with a slight change of dip direction near the corner of sections 8, 9, 16, and 17. A normal fault trends north-south near the south-east side of the survey area. Color bar is reflection time (ms).

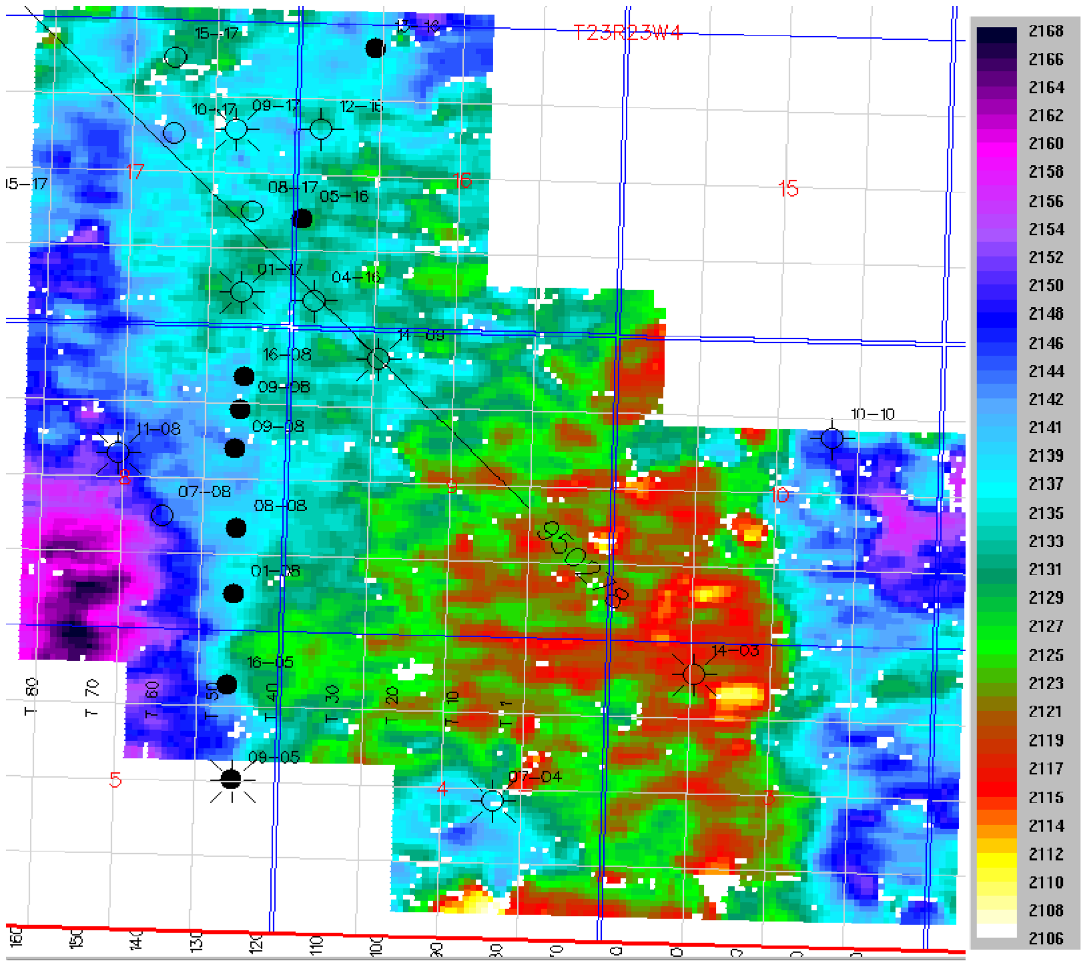

Fig. 5b. P-S time structure map, basal Cambrian time. The red/yellow area shows a horst block in the south-central part of the area. More local variations are visible than shown in figure 5a. Color bar is reflection time (ms).

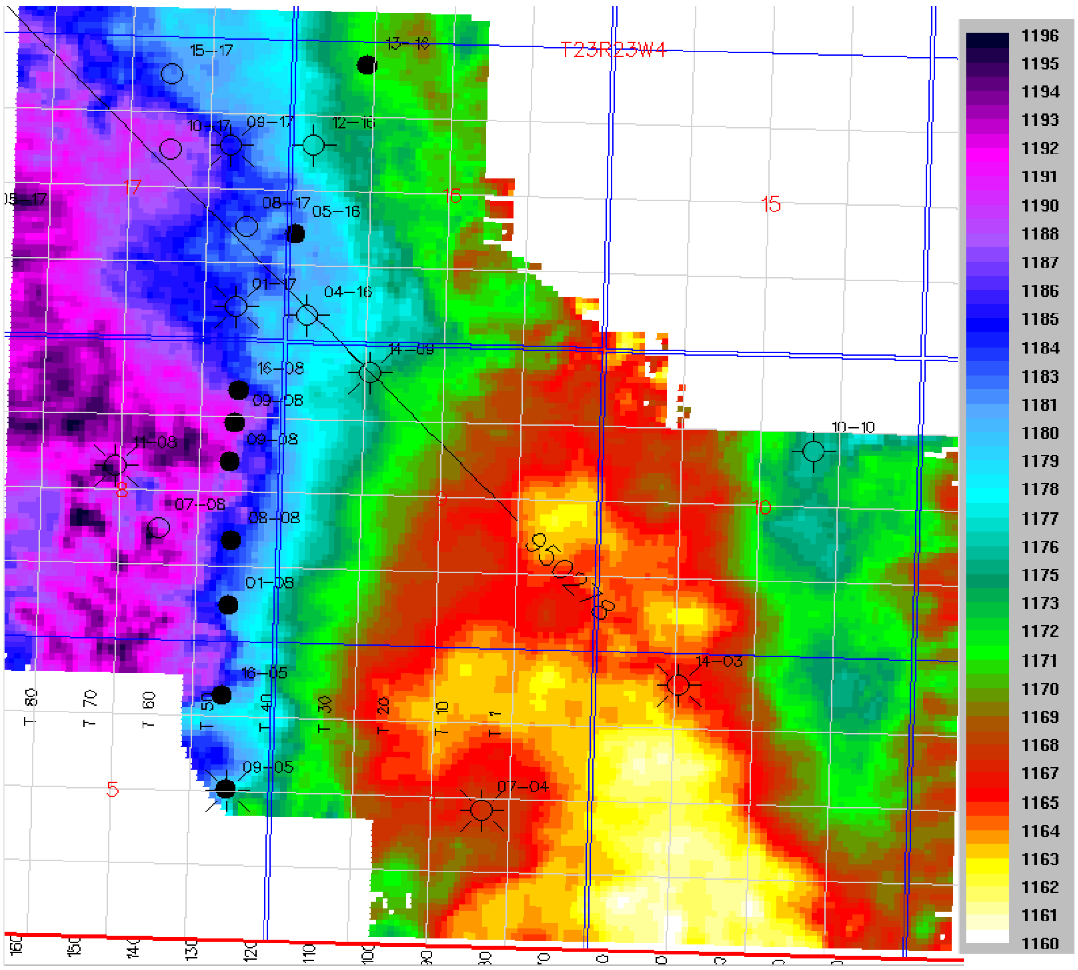

Fig. 6a. *P-P* time structure map, Wabamun event. Color bar is reflection time (ms).

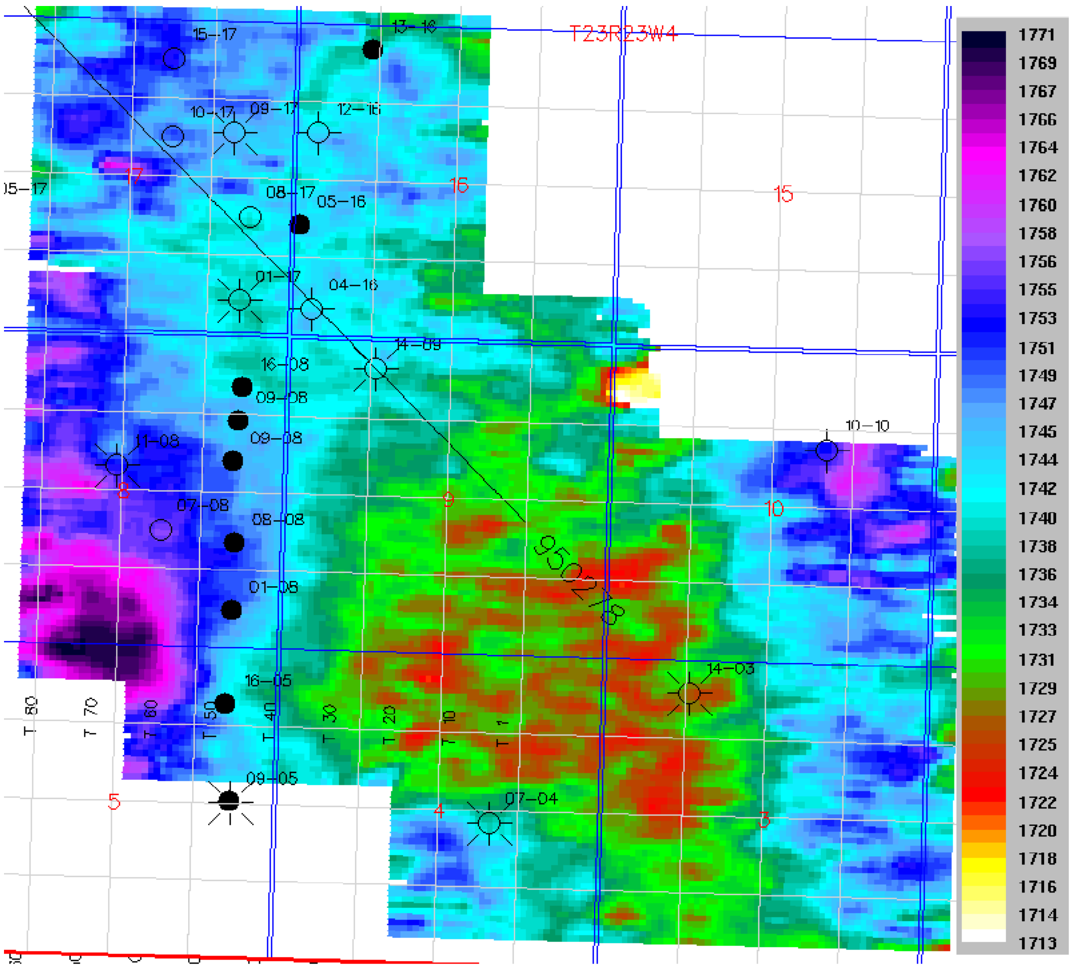

Fig. 6b. *P-S* time structure map, Wabamun event. Color bar is reflection time (ms).

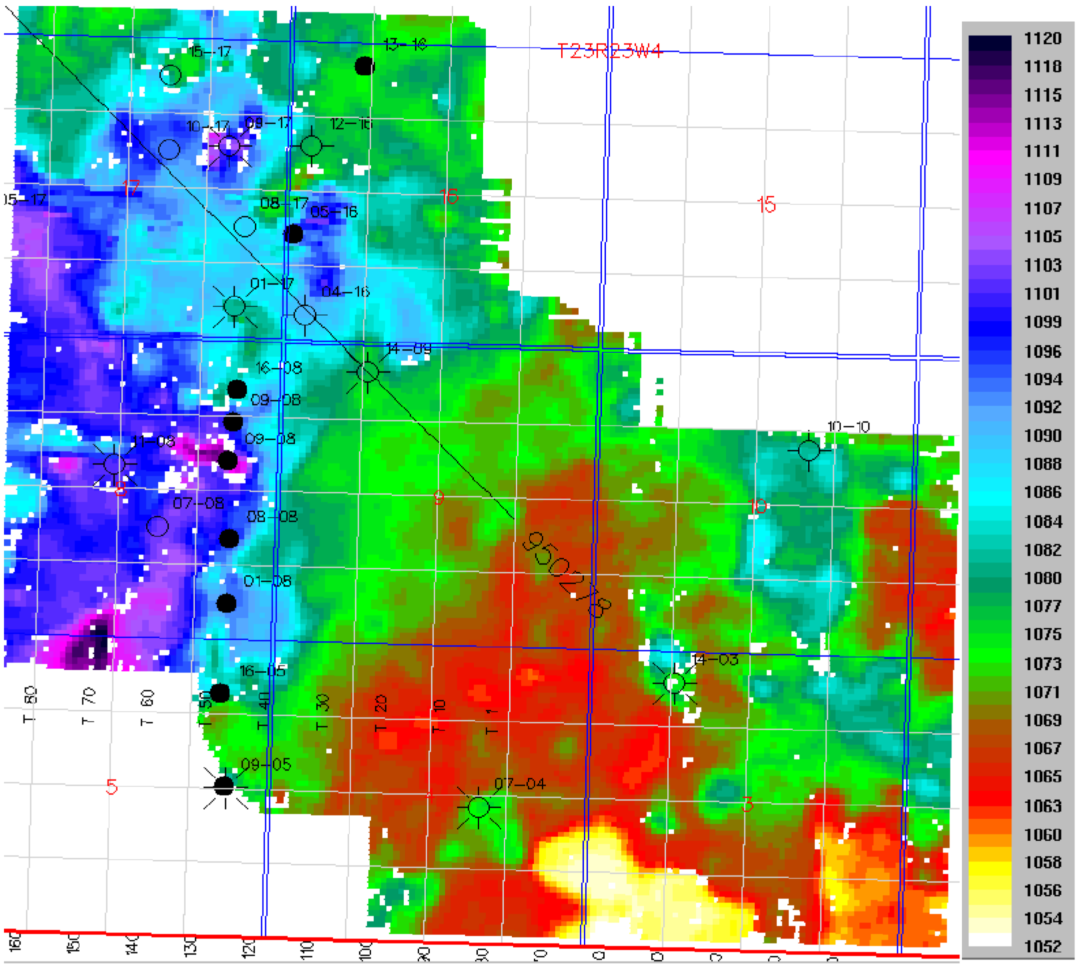

Fig. 7a. *P-P* time structure, Mississippian event. Color bar is reflection time (ms).

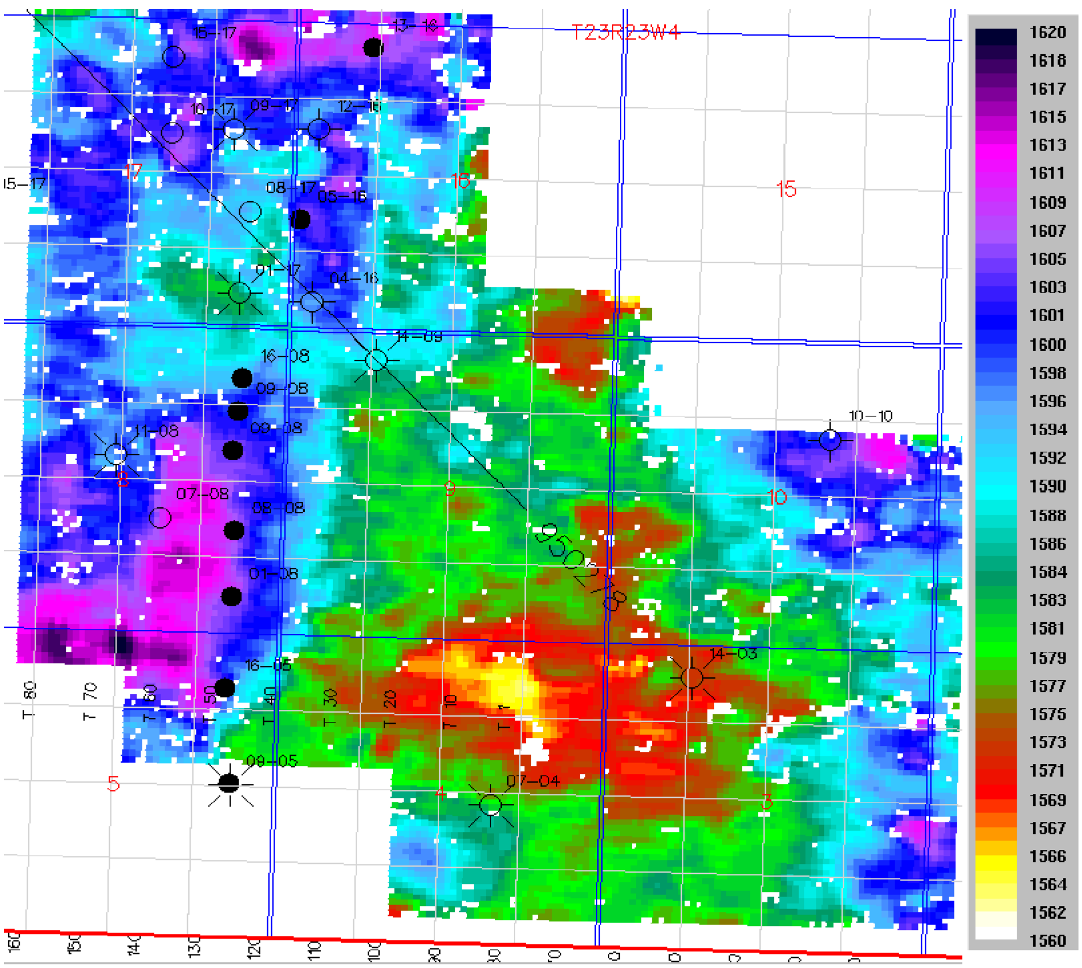

Fig. 7b. *P-S* time structure, Mississippian event. Note that the structural relief marked in green extends into section 17 through the corner of sections 8, 9, 16 and 17. Color bar is reflection time (ms).

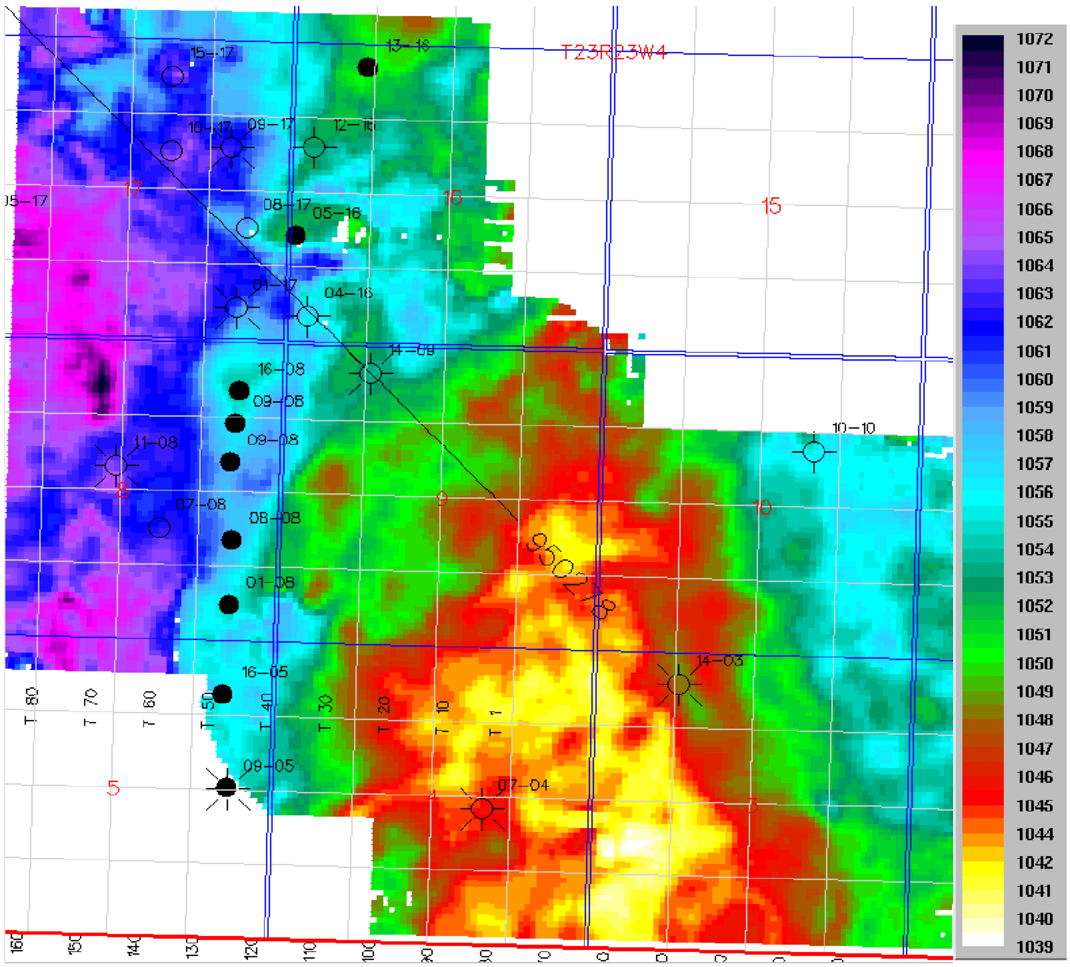

Fig. 8a. *P-P* time structure, top channel event. The red/yellow color zones indicate shorter traveltime or a structural high. Color bar is reflection time (ms).

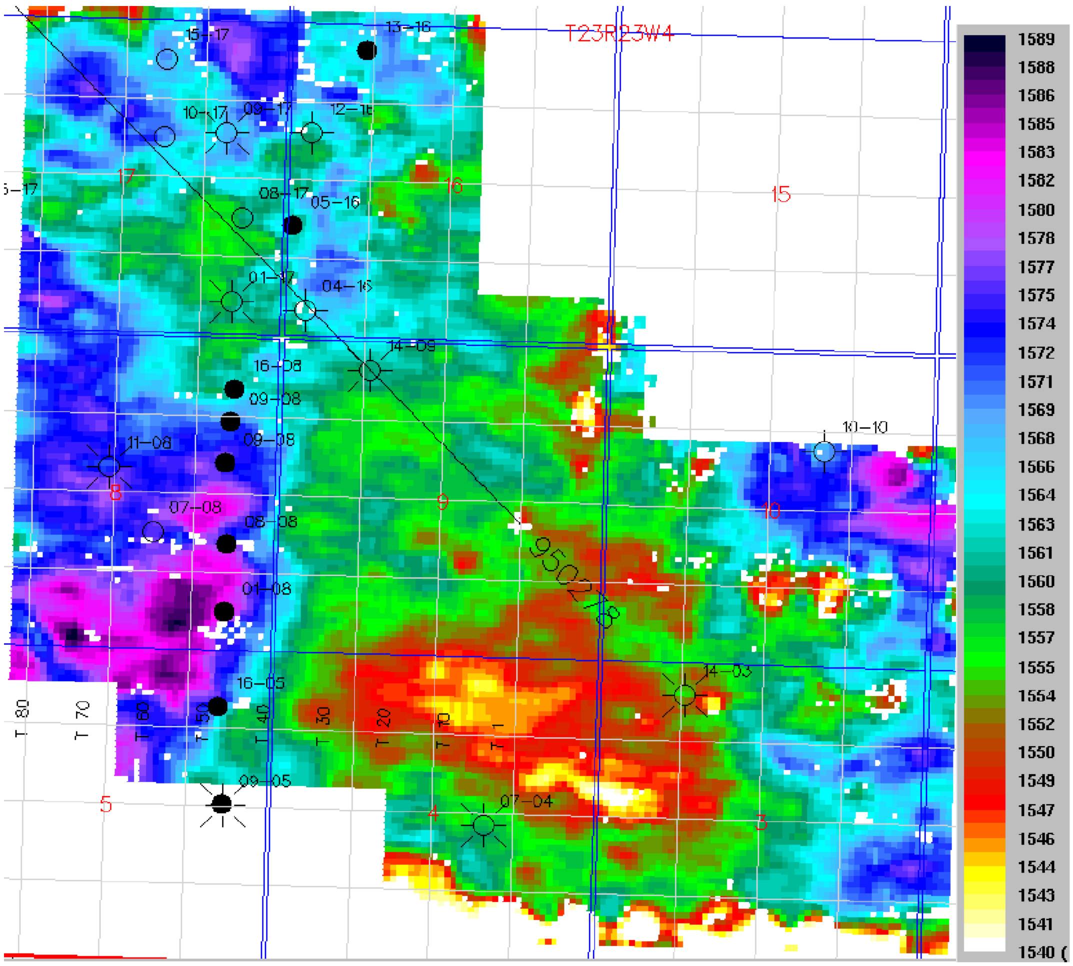

Fig. 8b. *P-S* time structure, top channel level. The greenish color (high relief) surrounded by the purple color (low in relief) in section 17 formed an updip seals for reservoirs in the south. Color bar is reflection time (ms).

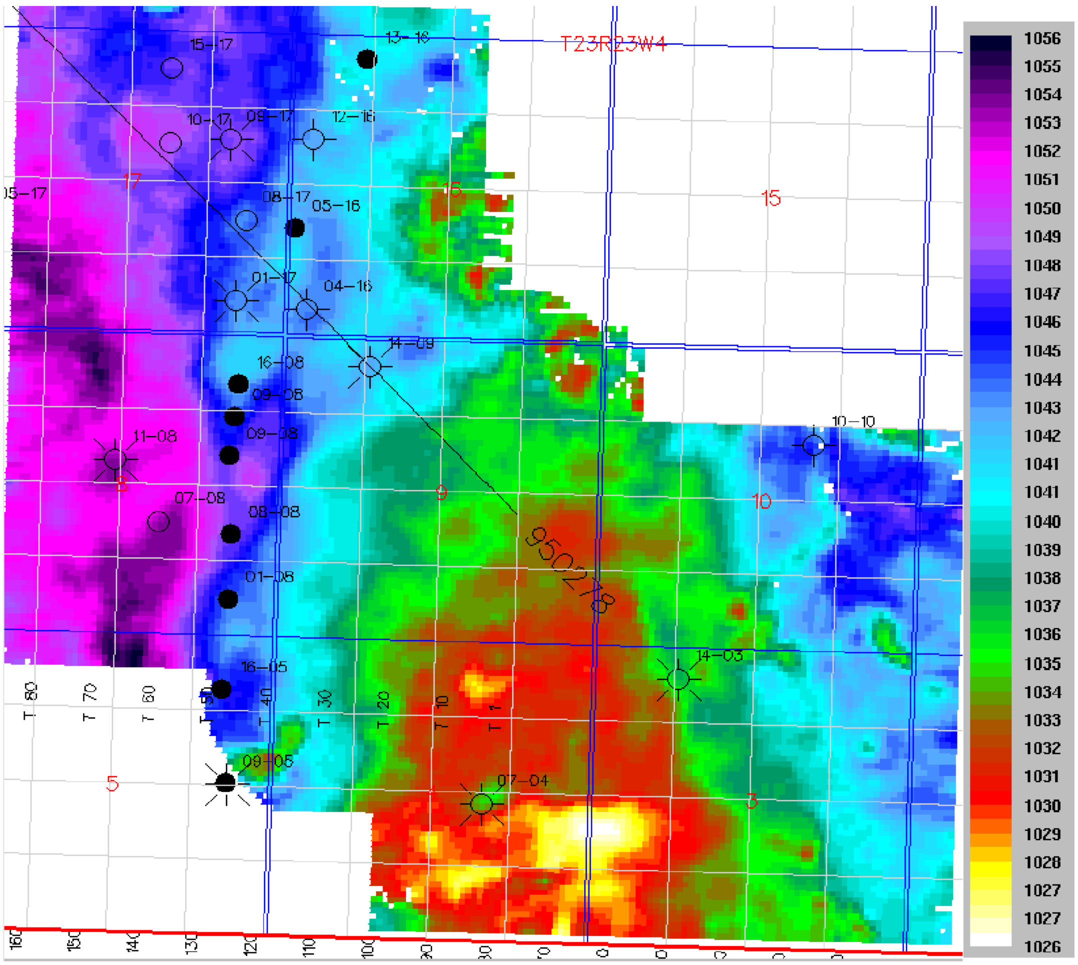

Fig. 9a. *P-P* time structure, Lower Mannville event, the red/yellow color zones indicate the structural high. Color bar is reflection time (ms).

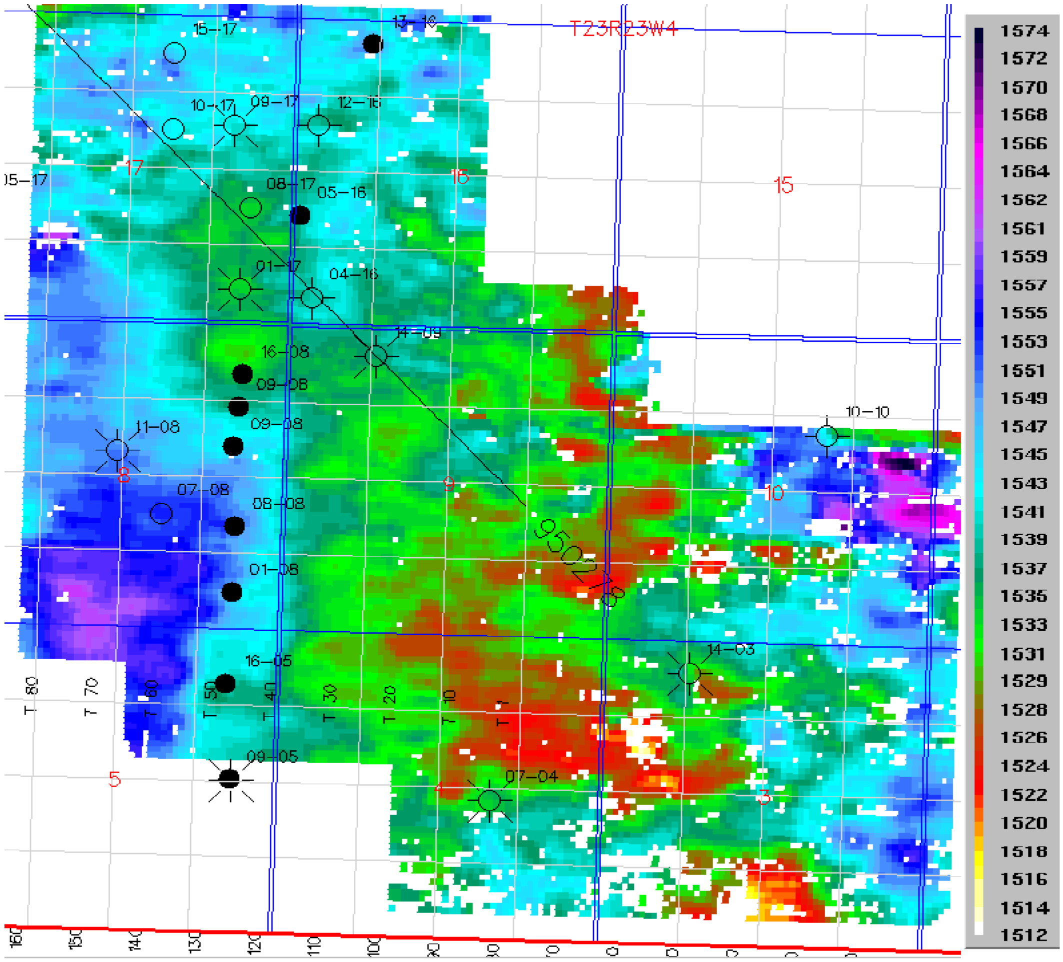

Fig. 9b. *P-S* time structure, Lower Mannville event. Color bar is reflection time (ms).

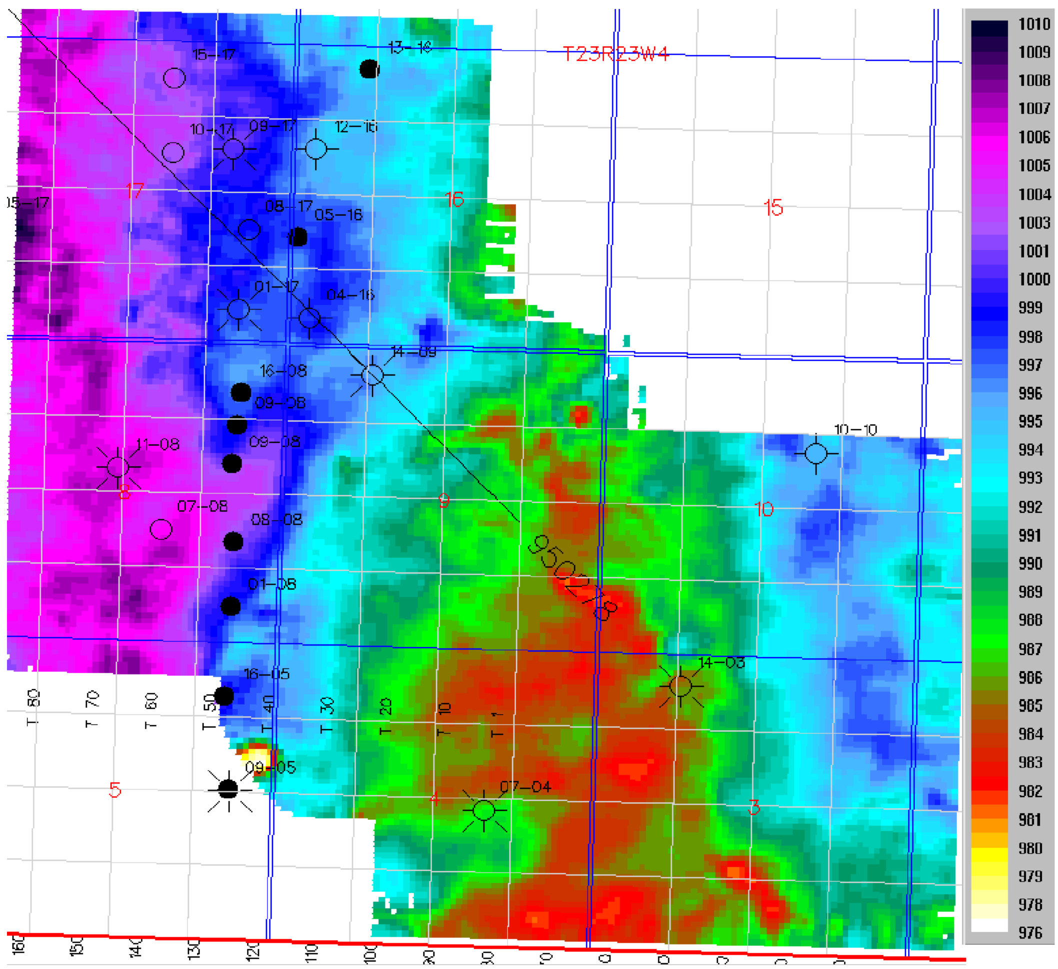

Fig. 10a. *P-P* time structure, Mannville event, the red/yellow color zones indicate the structural high. Color bar is reflection time (ms).

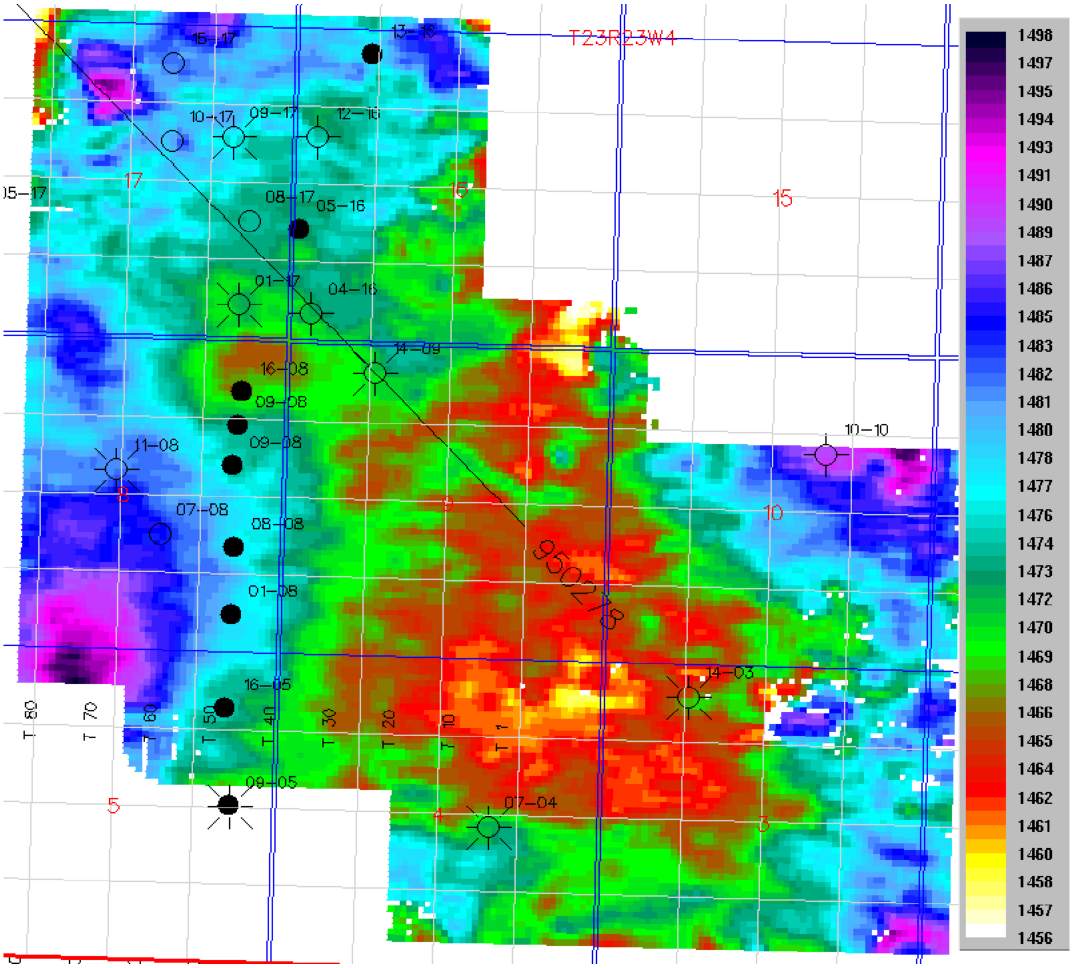

Fig. 10b. *P-S* time structure, Mannville event, the red/yellow color zones indicate the structural high. Color bar is reflection time (ms).

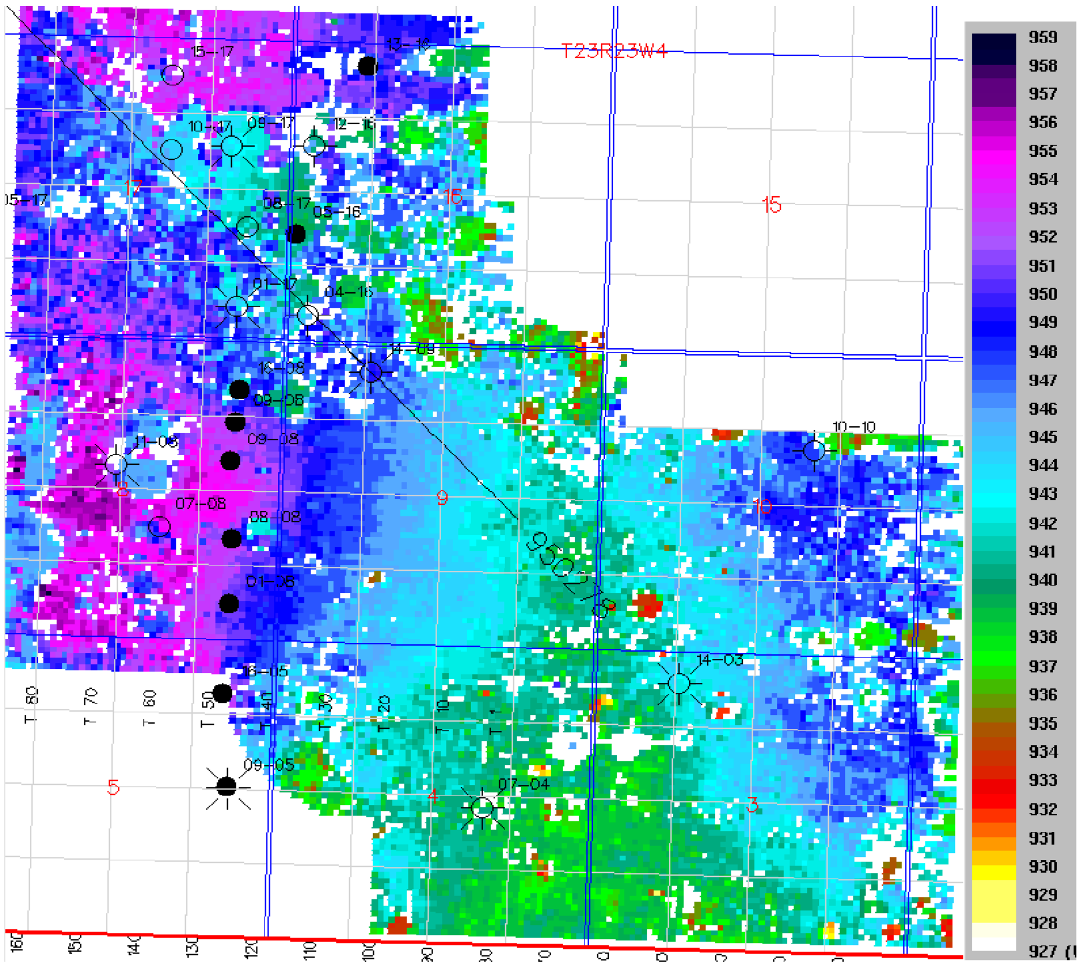

Fig. 11a. *P-P* time structure, Viking event. Color bar is reflection time (ms).

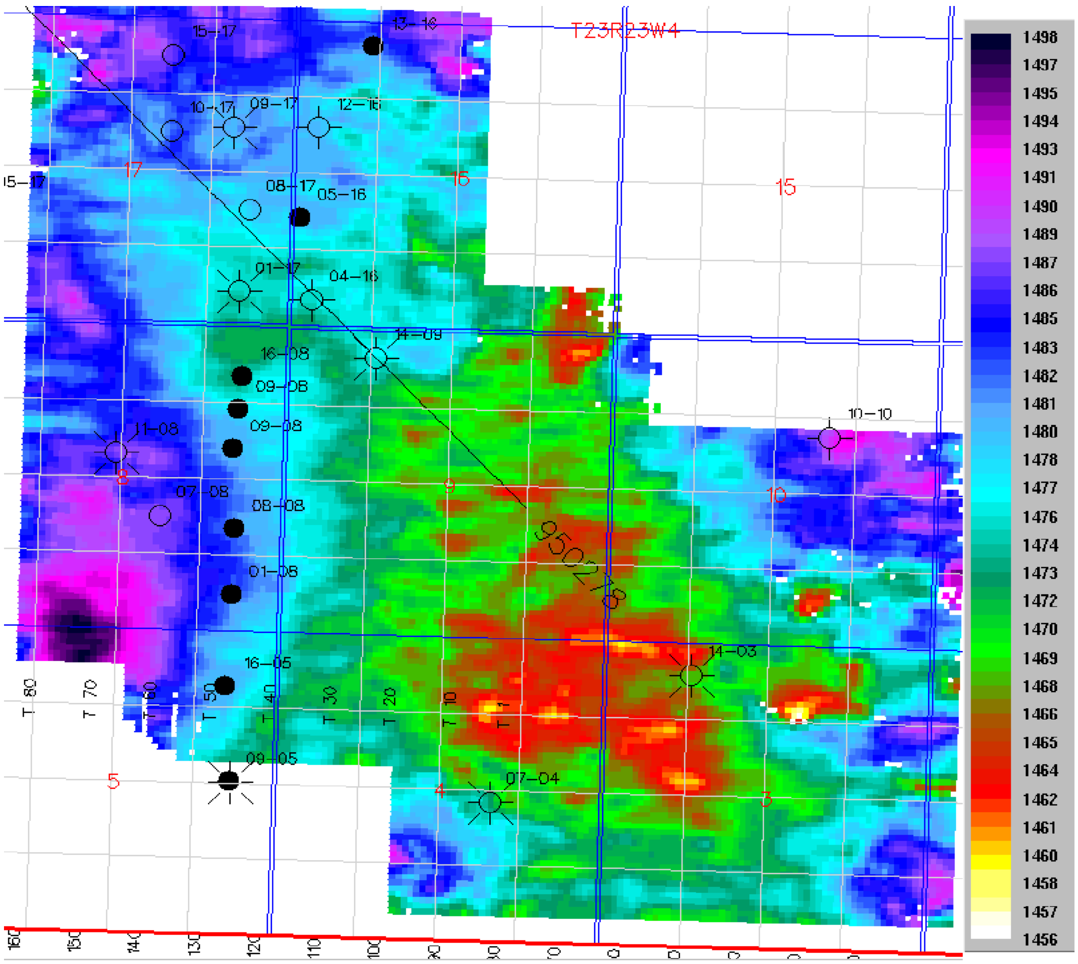

Fig. 11b. *P-S* time structure, Viking event. Color bar is the reflection time (ms).

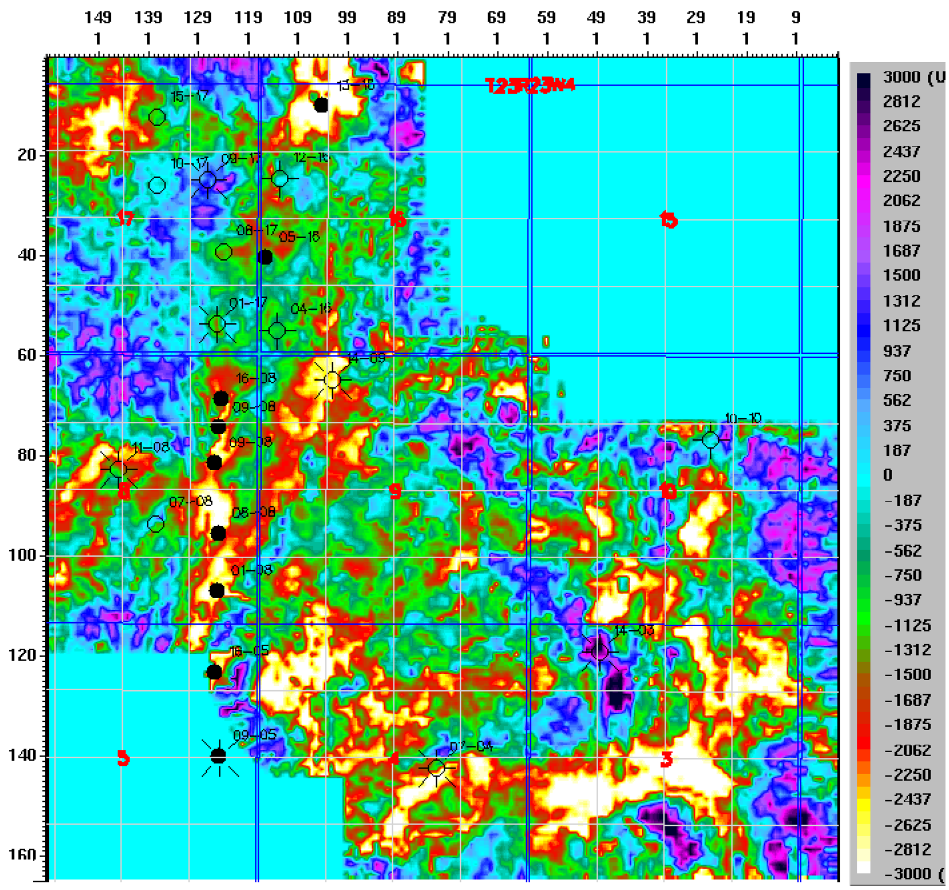

Fig. 12a. *P-P* time slice at 1054 ms (flattened at Mannville). This time slice cuts the volume at about the level of the channel. The color bar represents seismic reflection amplitude.

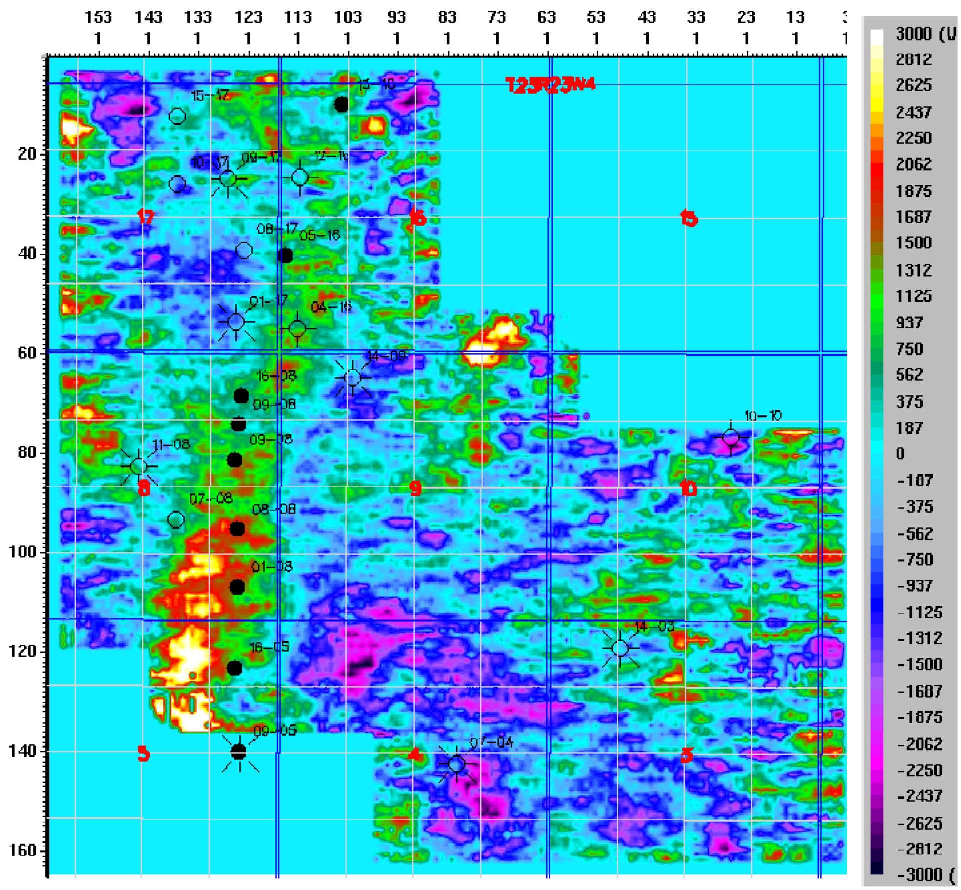

Fig. 12b. *P-S* time slice section at 1560 ms (flattened at Mannville), equivalent to the level of the channel. One can clearly see the yellow/reds extend in the north-south direction across the left central half of the image. The progressively darker reds indicate strengthening of the seismic amplitude and the areas of color yellow have the strongest seismic amplitude. Reds/yellows and greens are seismic peaks and troughs. The Glauconitic channel (or valley) has low sinuosity with an estimation of width near 400 m. Regional wells lie outside this interpreted channel trend.

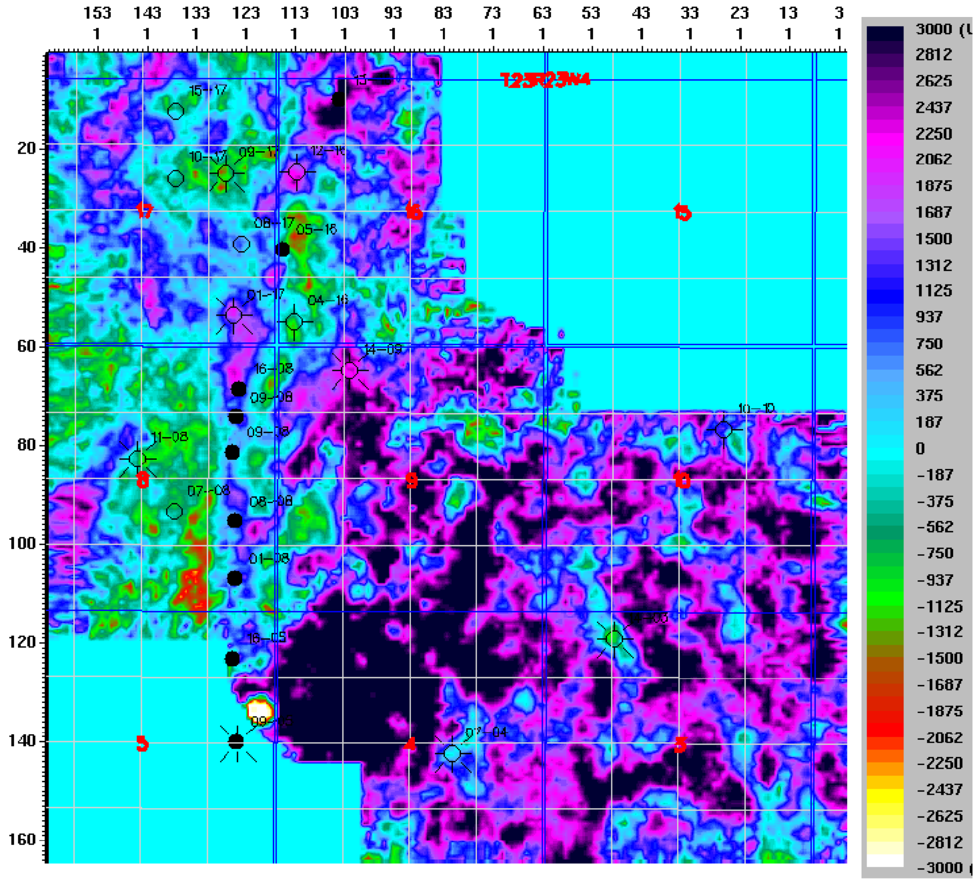

Fig. 13a. *P-P* time slice section at 1080 ms (flattened at Mannville). This time slice cuts the volume at about the level of a possible Detrital channel just above the Mississippian surface.

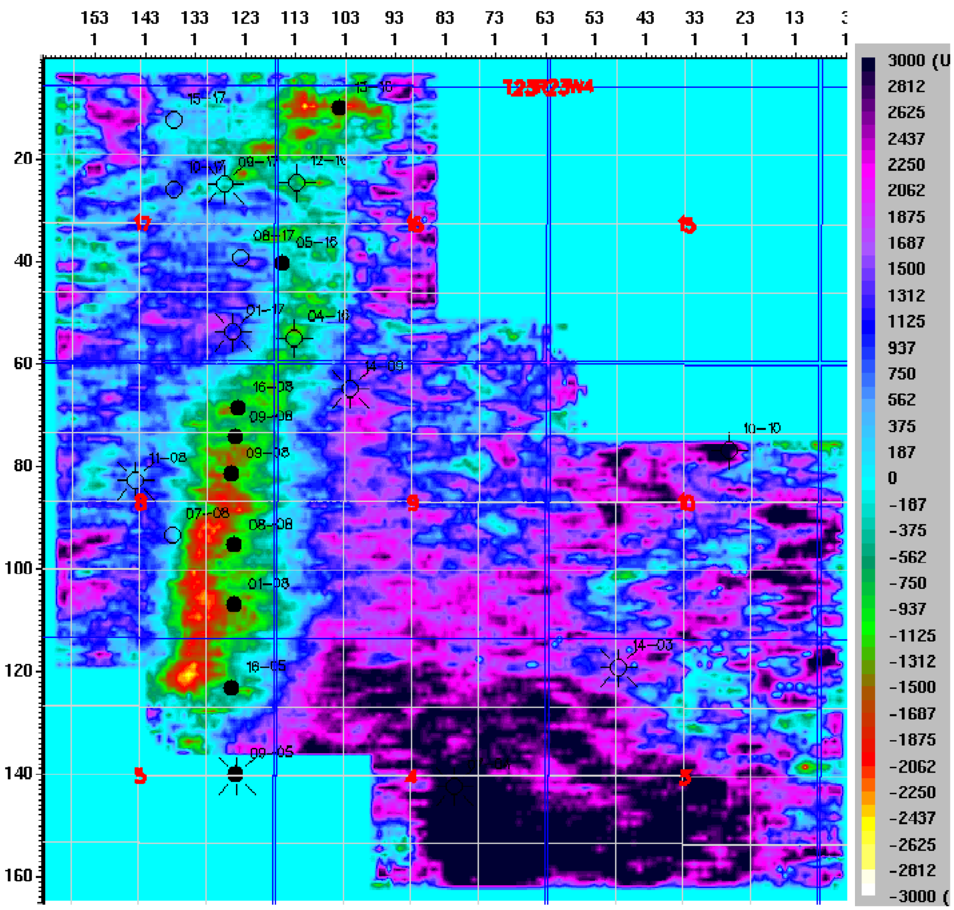

Fig. 13b. *P-S* time slice section at 1590 ms (flattened at Mannville), equivalent to the level of a channel just above the Mississippian surface. The greenish color running north-northeast to south on the left part of the image is evident. Color bar is amplitude.

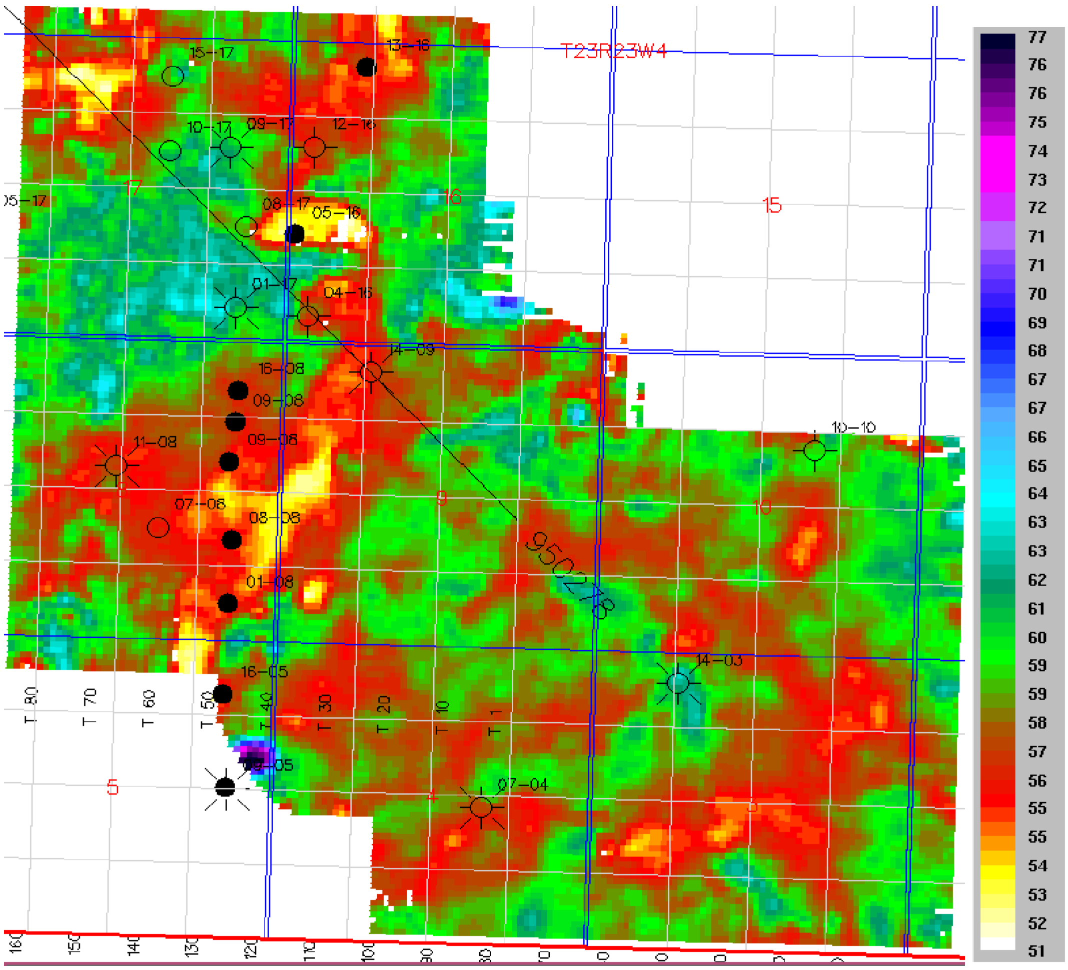

Fig. 14a. *P-P* isochron from Mannville to top channel events. Color bar is traveltime (ms).

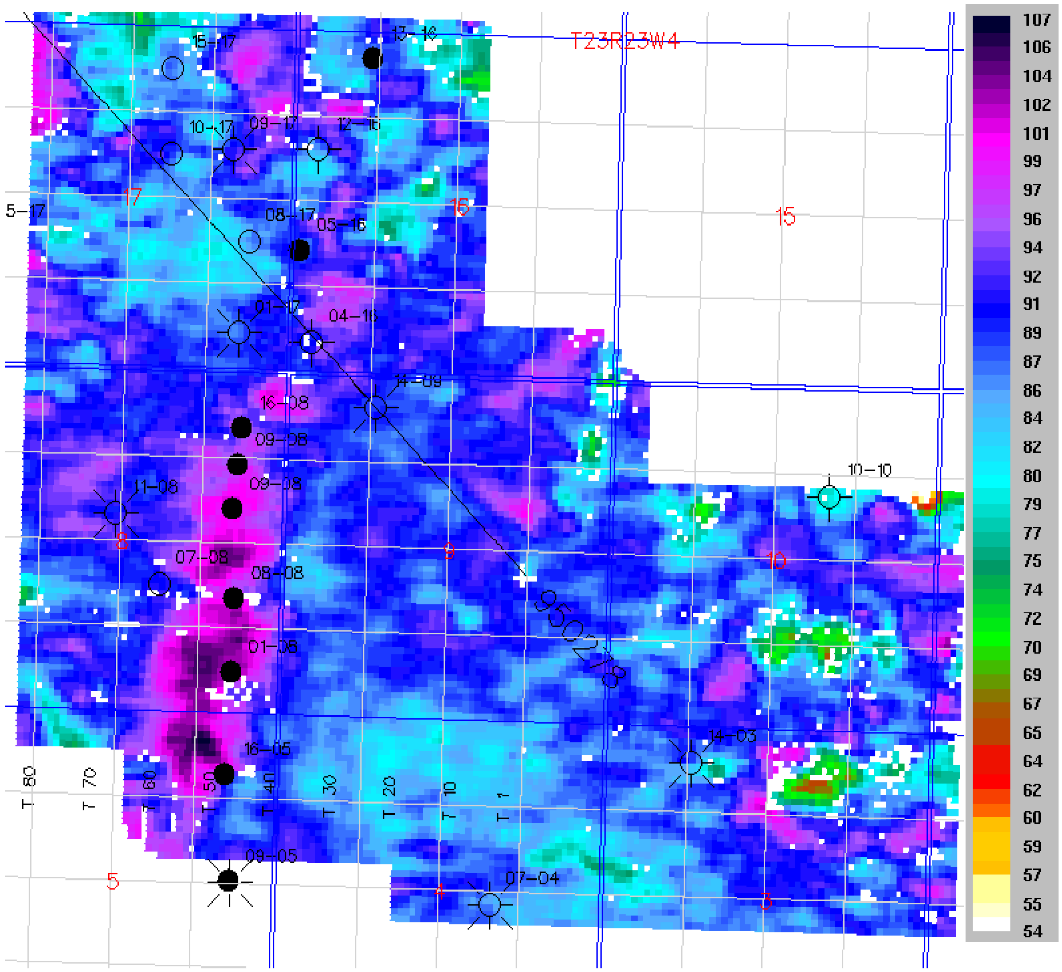

Fig. 14b. *P-S* isochron from Mannville to Top Channel event. Color bar is traveltime (ms).

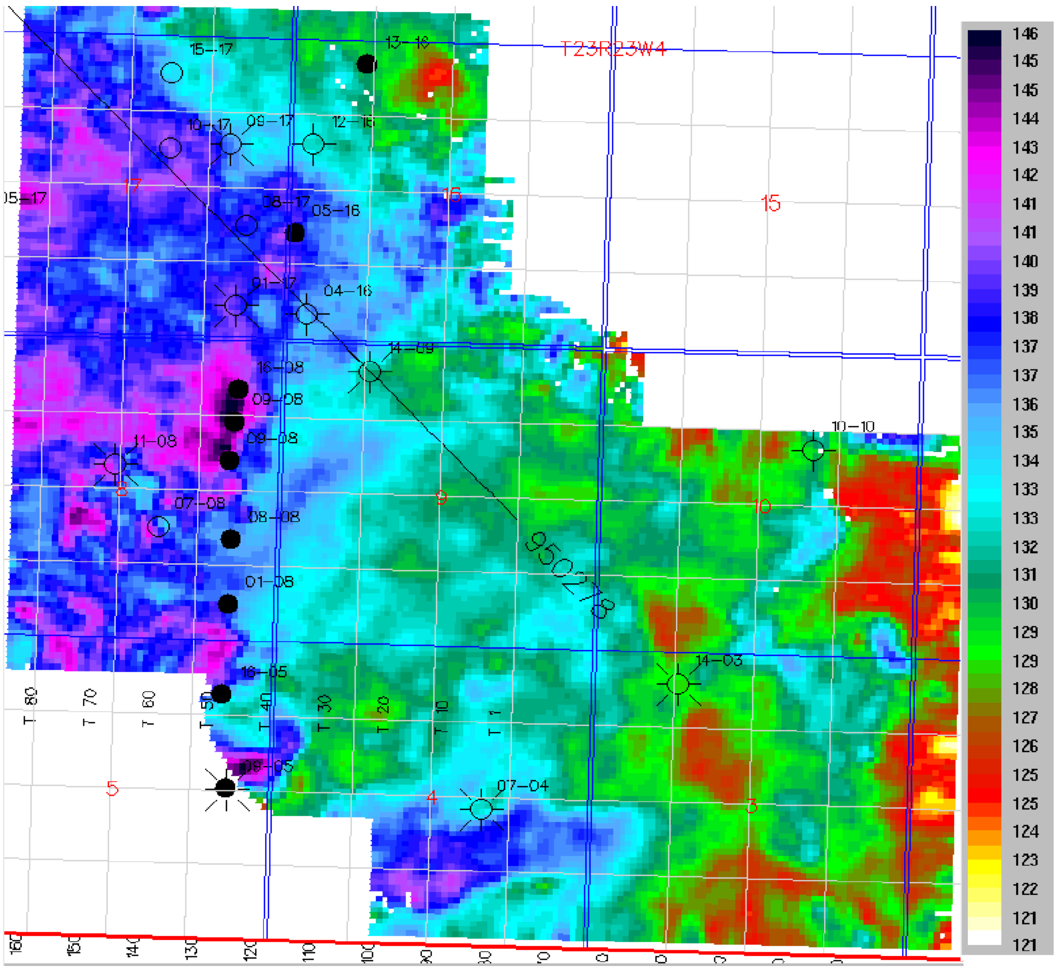

Fig. 15a. *P-P* isochron map from Wabamun to Lower Mannville event. Color bar represents traveltime (ms).

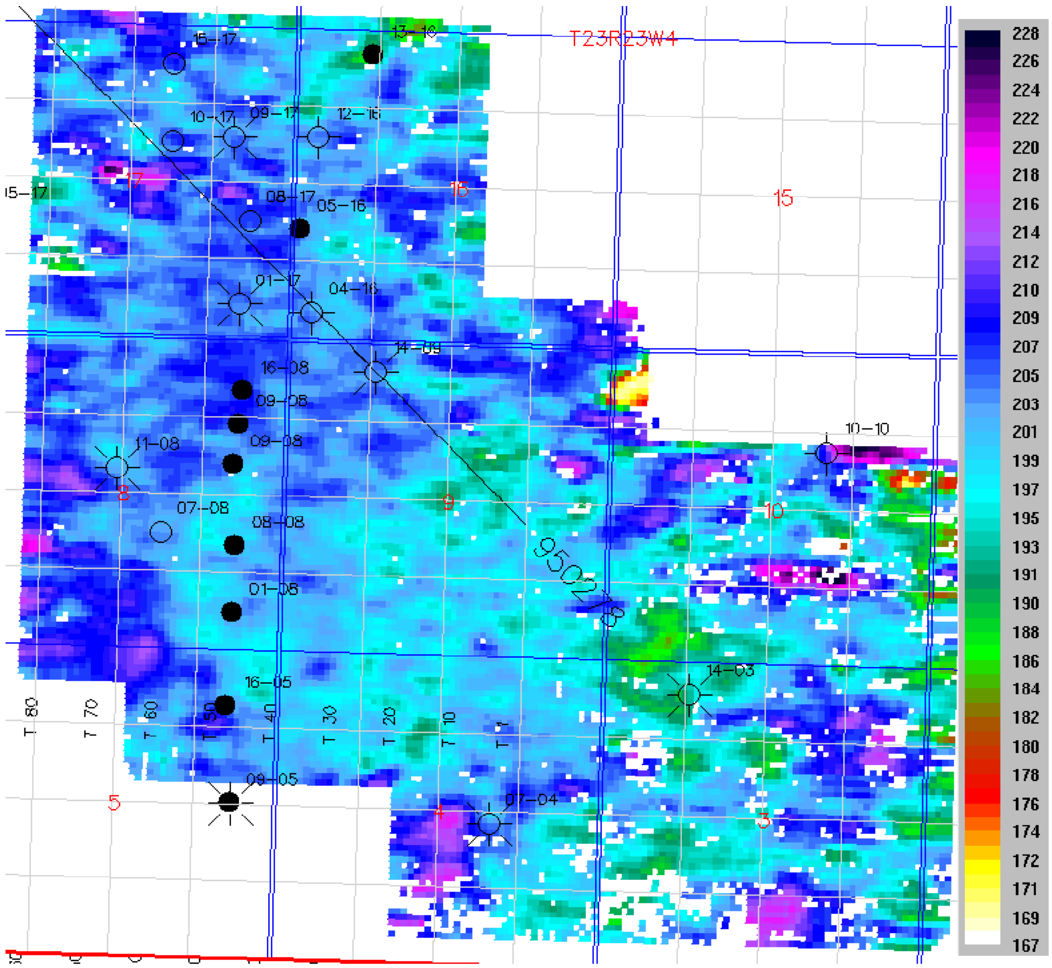

Fig. 15b. *P-S* isochron map from Wabamun to Lower Mannville. Note the thickness trend running north-south direction. Color bar represents traveltime (ms).

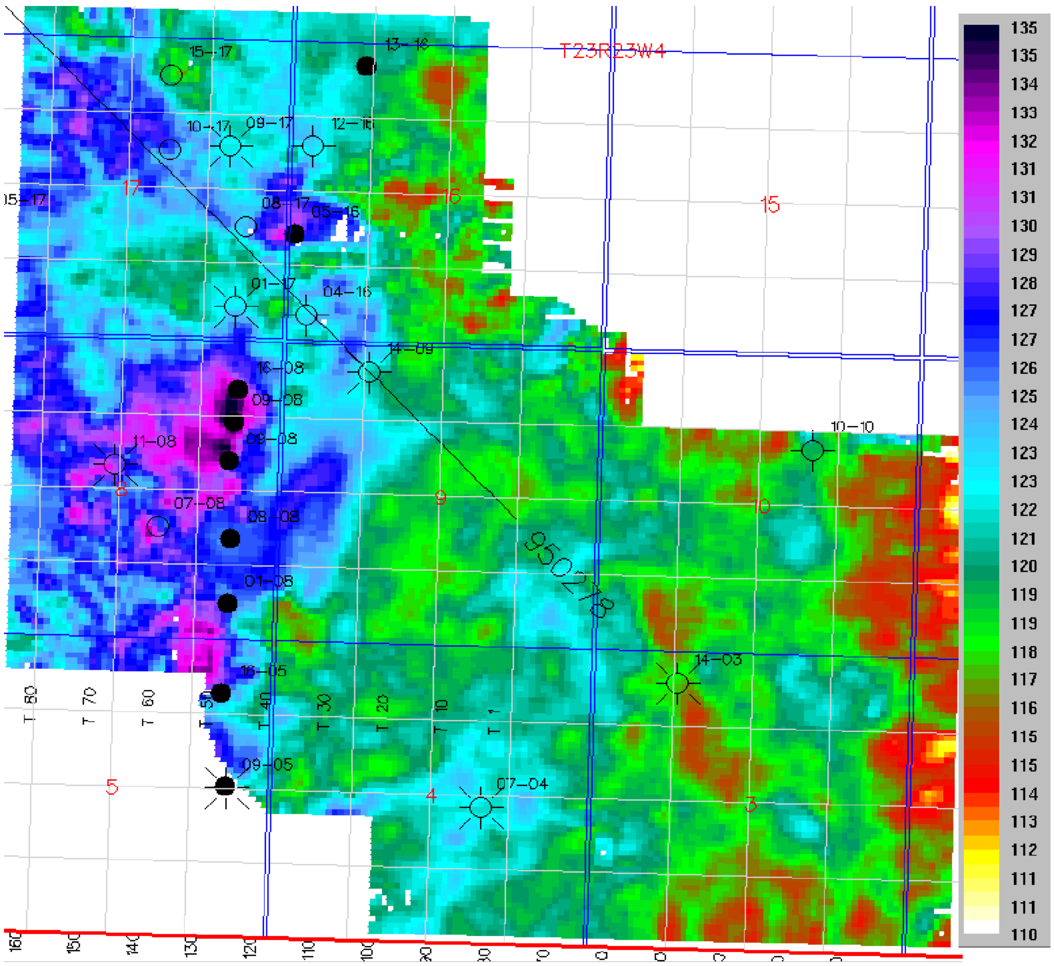

Fig. 16a. *P-P* isochron map from Wabamun to Top channel event. Color bar is traveltime (ms). The red/yellow color of smaller values indicate thinning.

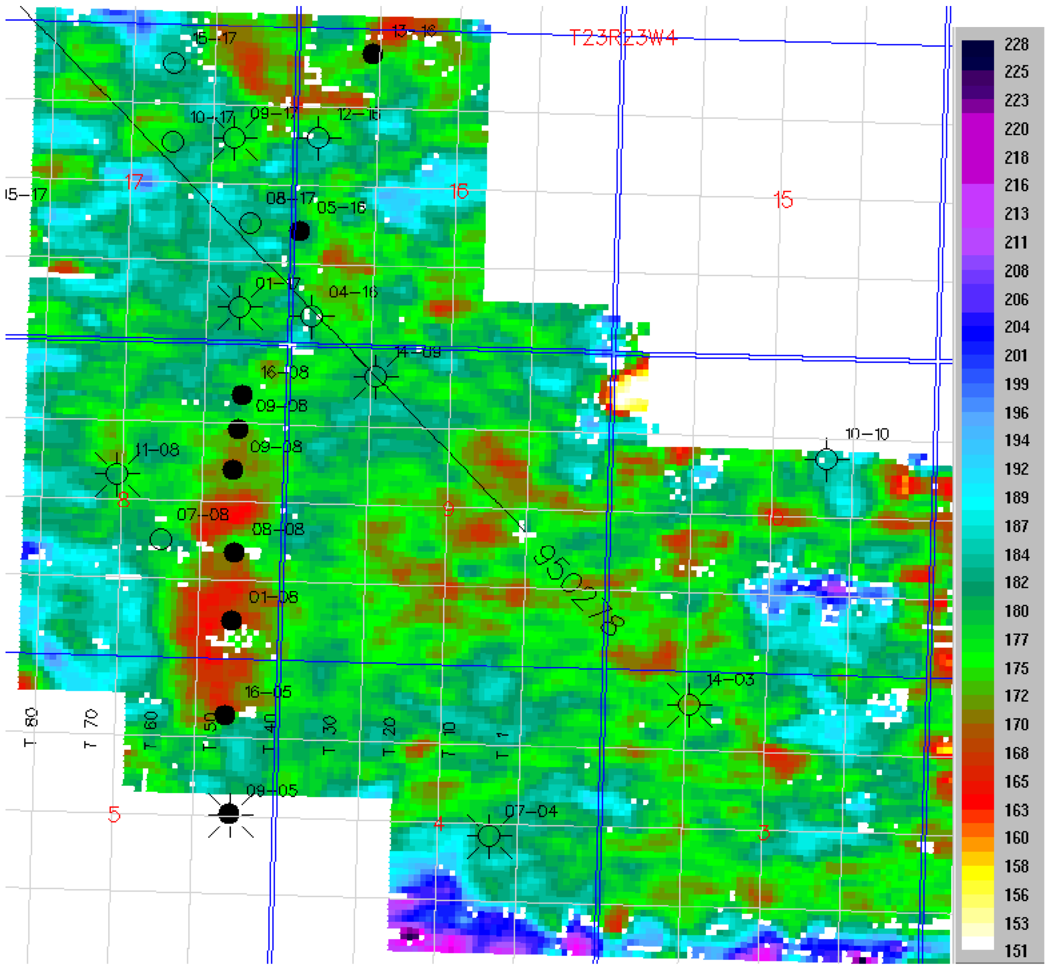

Fig. 16b. *P-S* isochron map from Wabamun to Top Channel event. Color bar is traveltime (ms). The red/yellow color of smaller values indicate thinning.

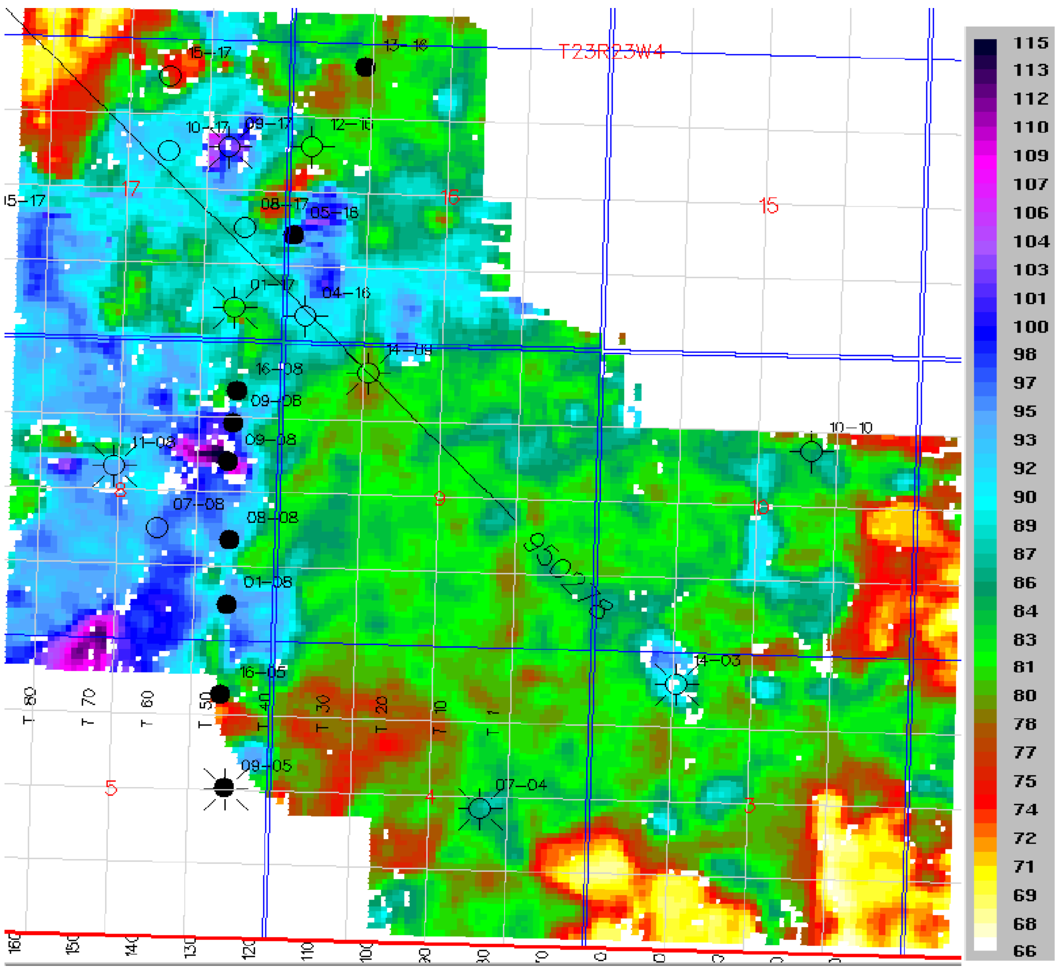

Fig. 17a. *P-P* isochron map from Mississippian to Mannville event. Color bar is the traveltime (ms). The red/yellow color of smaller values indicate thinning.

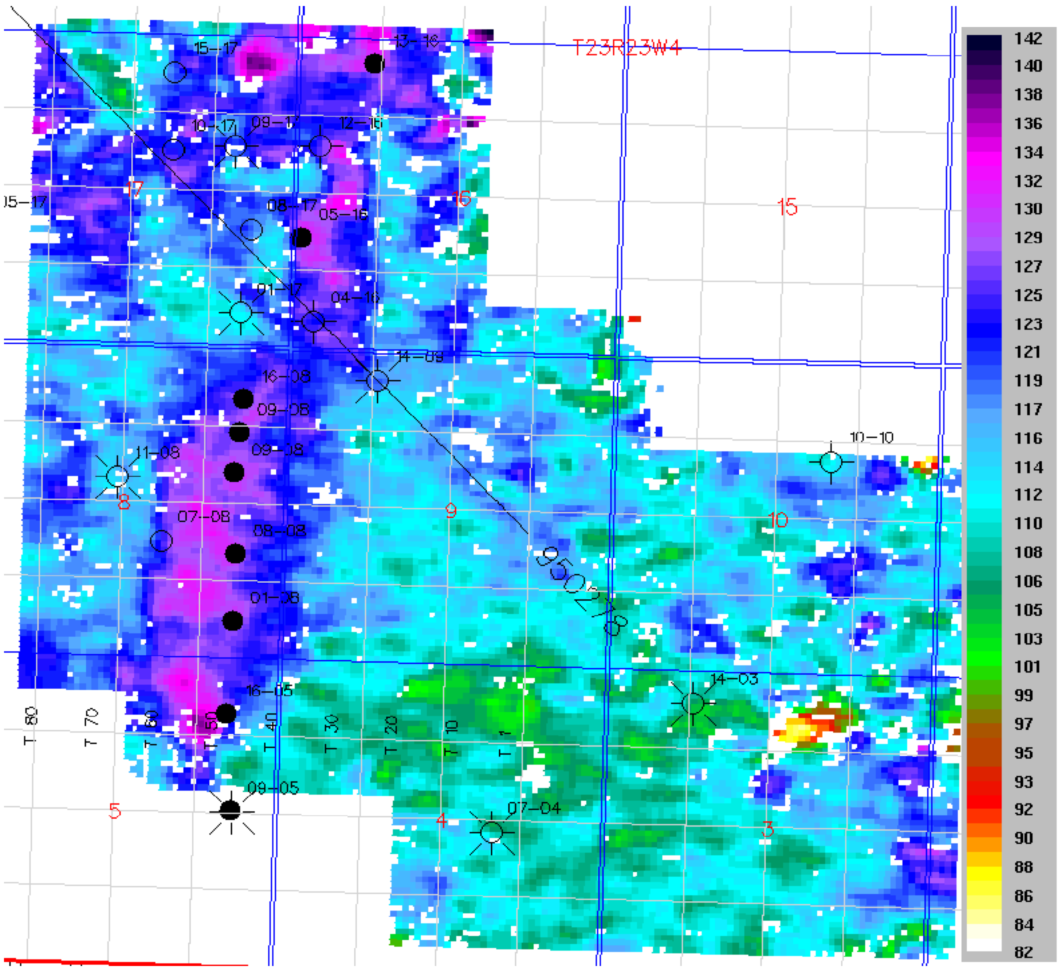

Fig. 17b. *P-S* isochron map from Mississippian to Mannville event. Color bar is traveltime (ms). The red/yellow color of smaller values indicate thinning.

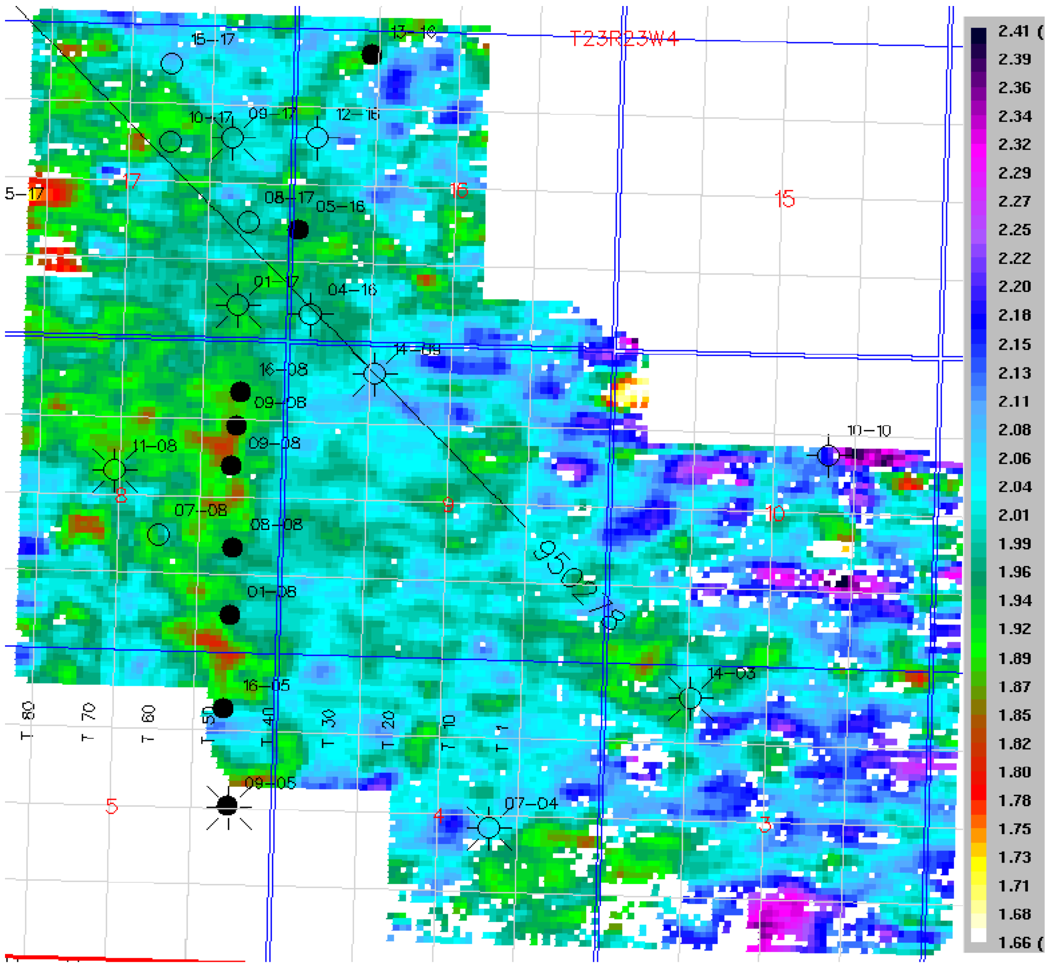

Fig. 18a *Vp /Vs* map, Lower Mannville - Wabamun , showing that the oil wells lie within the smaller *Vp/Vs* values of red / green color zone, while the 12-16 and 04-16 dry holes lie within the larger *Vp /Vs* value zone of blue color zone

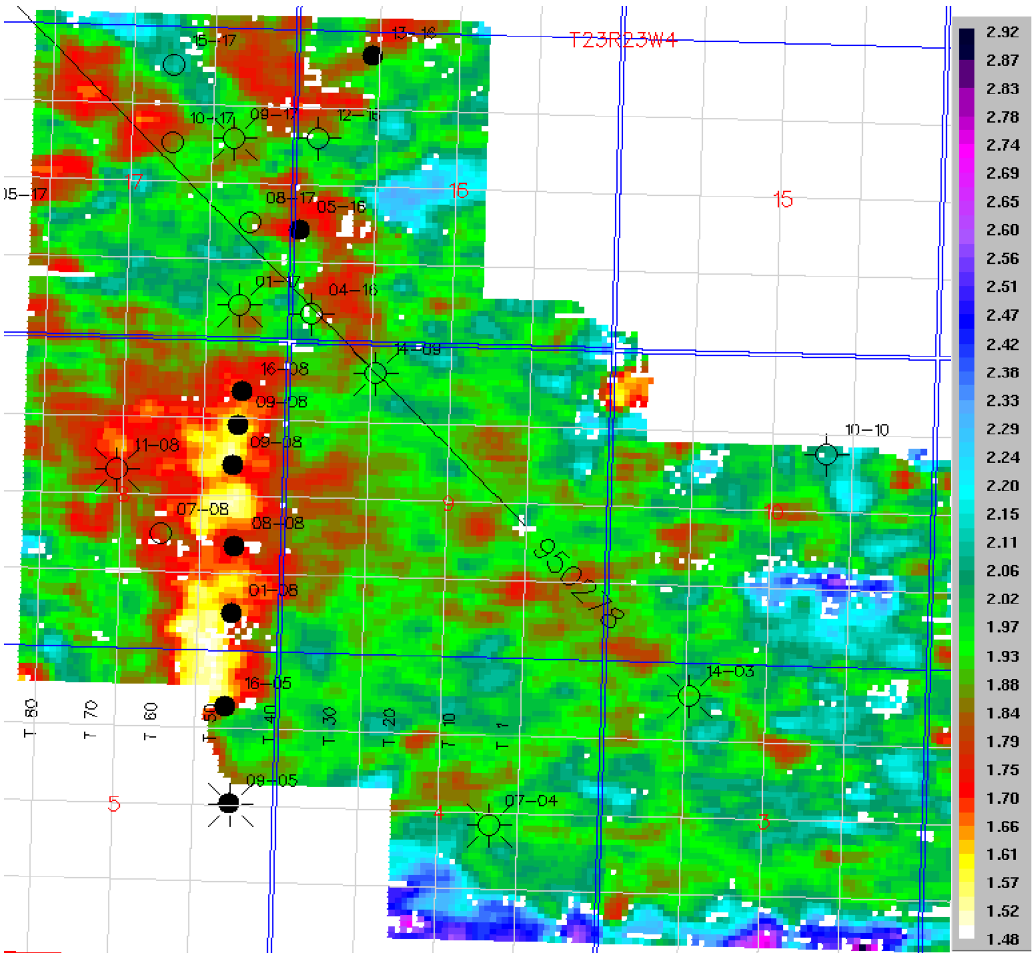

Fig. 18b. *Vp /Vs* map, top channel event - Wabamun , showing that the oil wells lie within the smaller *Vp /Vs* values of red / green color zone, while the 12-16 and 04-16 dry holes lie within the larger *Vp /Vs* value zone of blue color zone

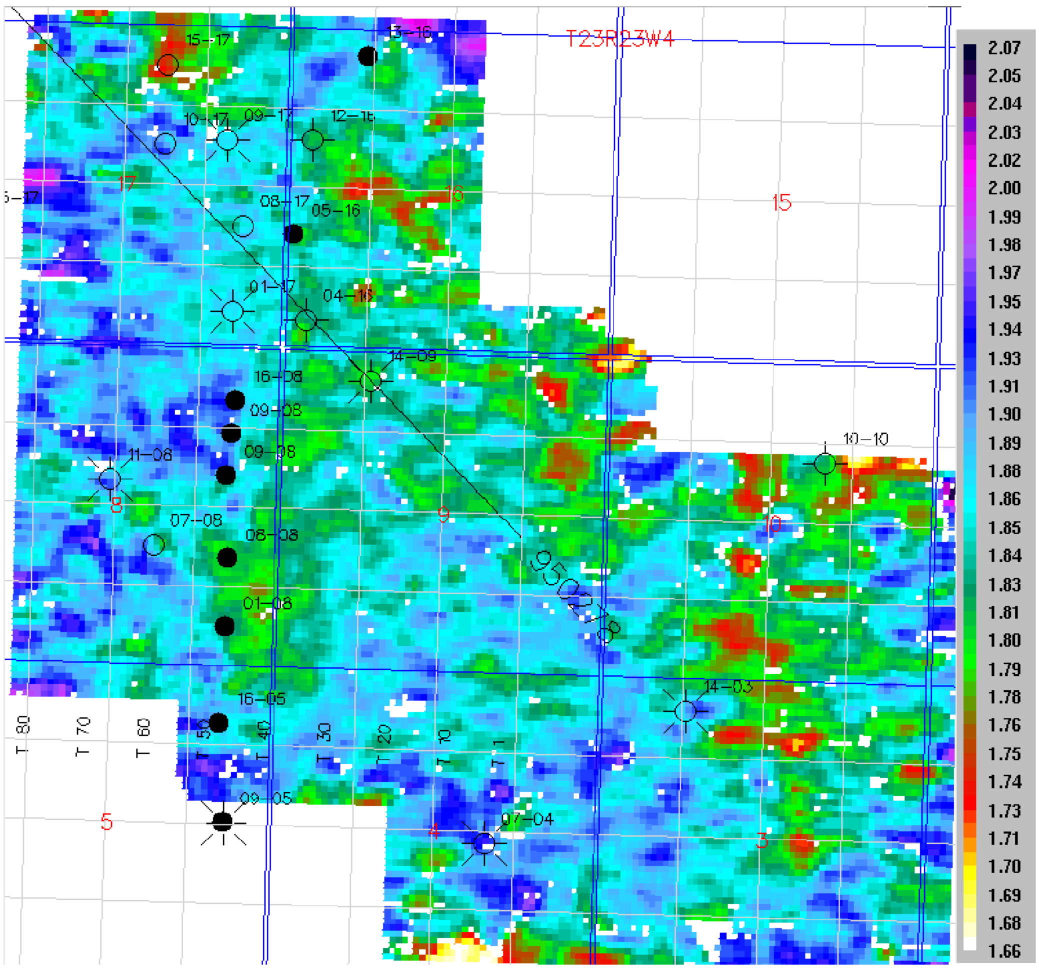

Fig. 18c. *Vp /Vs* map, basal Cambrian time - Wabamun , showing lower *Vp/Vs* values along the margins of the horst block.

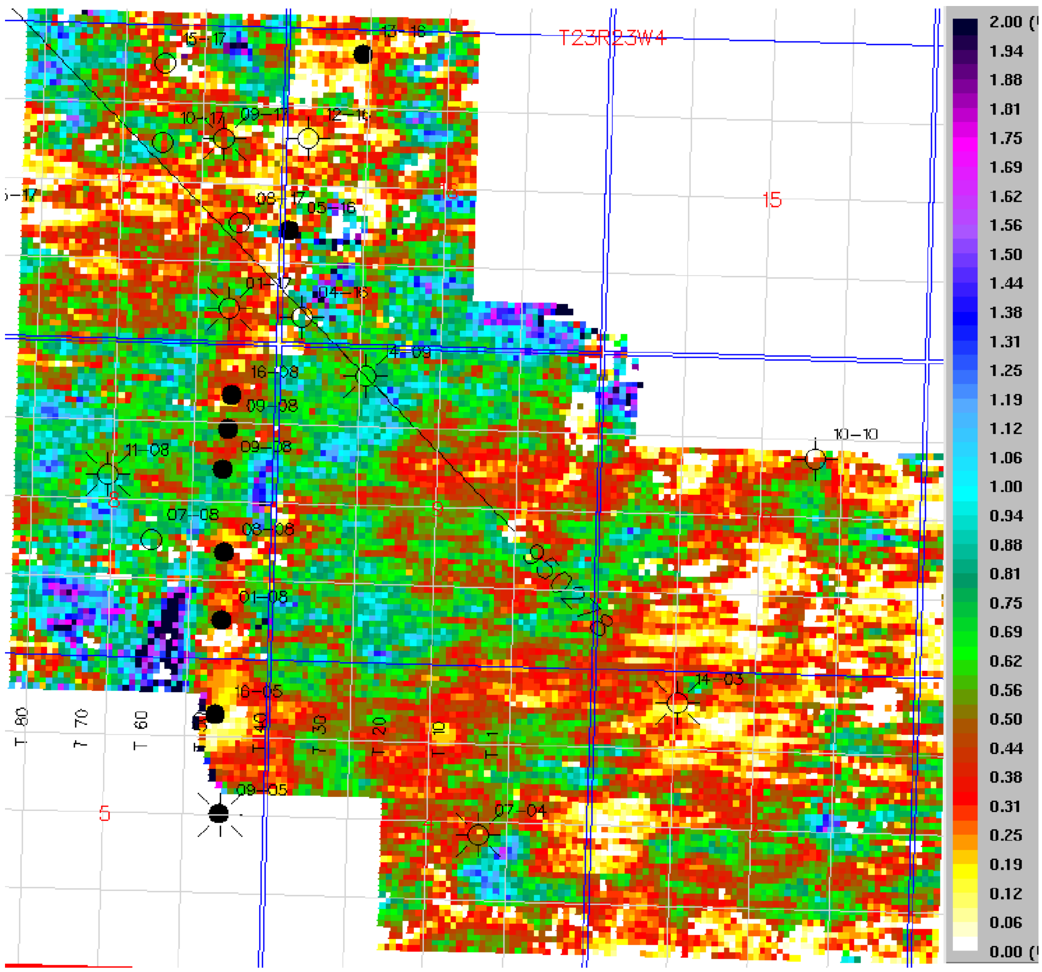

Fig. 19a Amplitude ratio of *P-S* versus *P-P* on Top Channel event

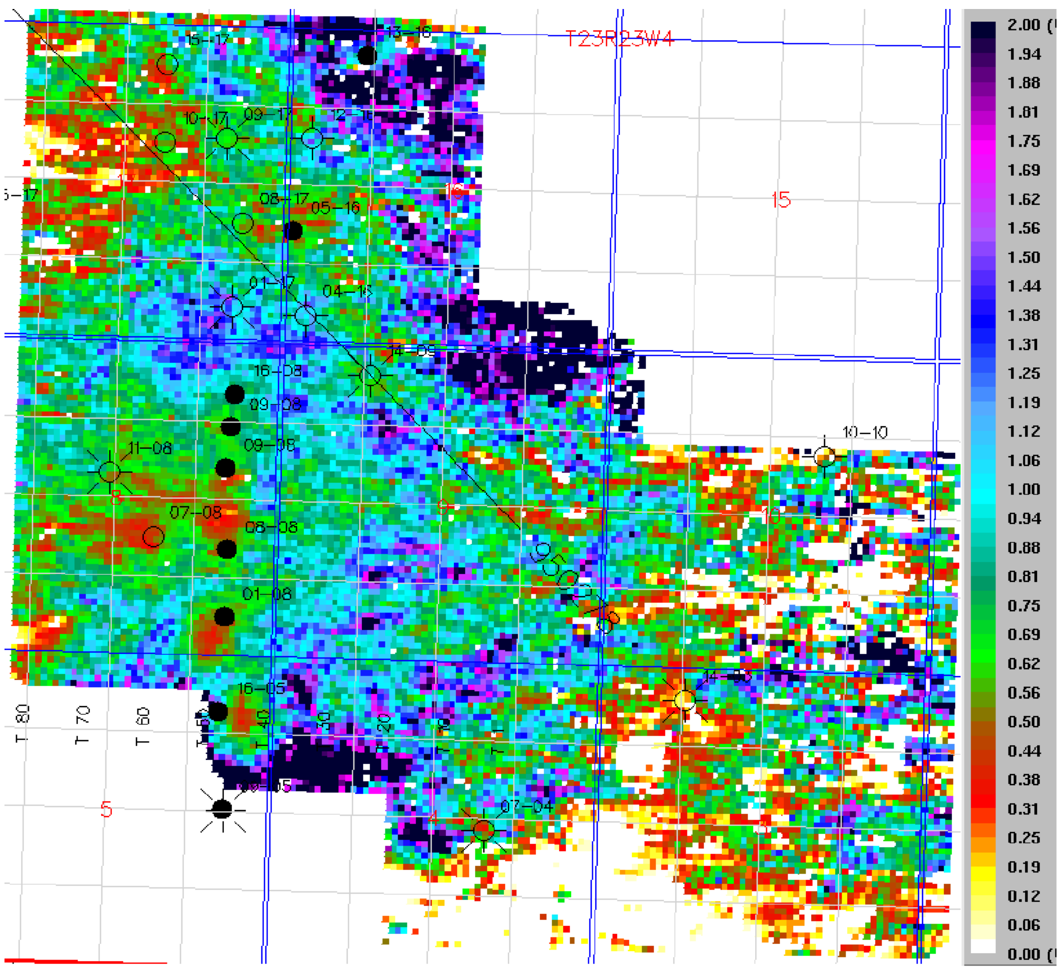

Fig. 19b. Amplitude ratio of *P-S* versus *P-P* on Lower Mannville event. The bluish purple color indicates the *P-S* amplitude is higher than the *P-P* amplitude.

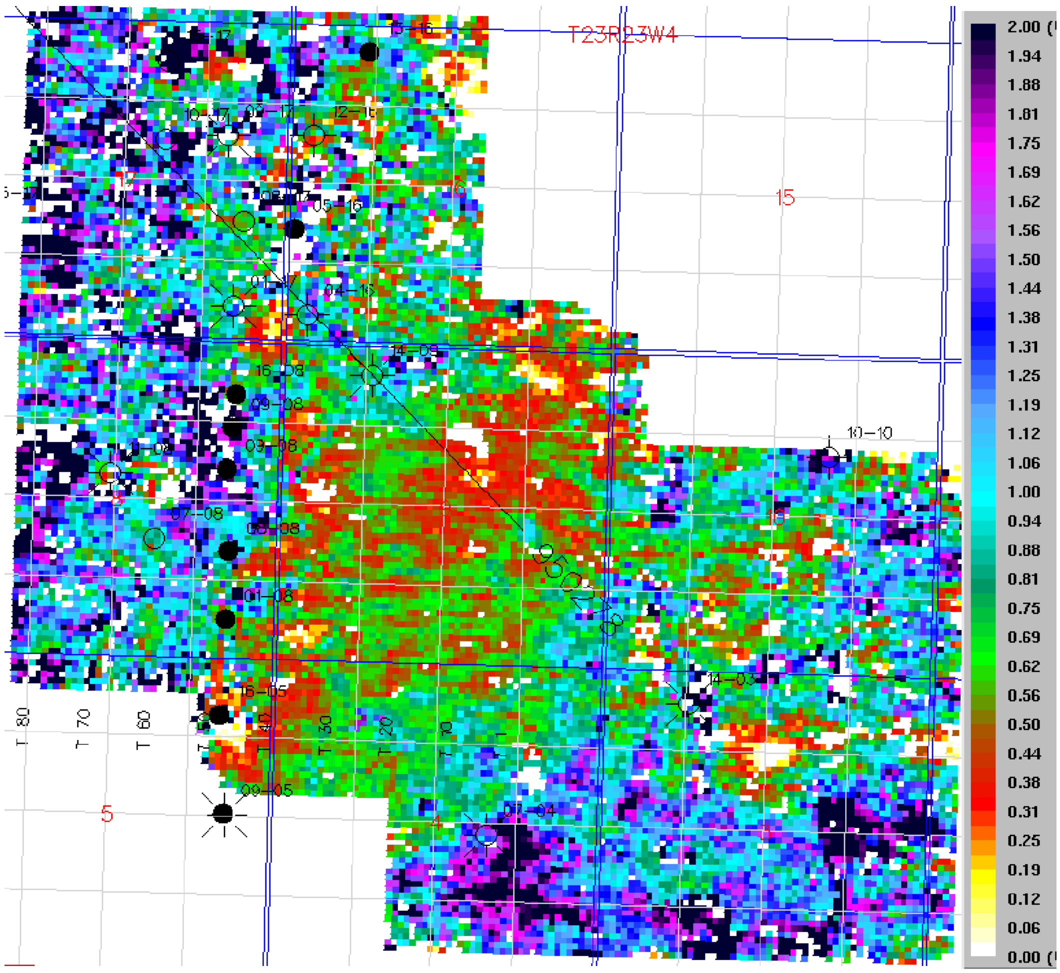

Fig. 19c. Amplitude ratio of *P-S* versus *P-P* on Mississippian event. Note that in the central part of the survey area, *P-S* amplitude is less than *P-P* amplitude. The edge coincides with the well controls, is it where the lithology changes from sand to shale?

Twp. 23 Rge. 23 W4

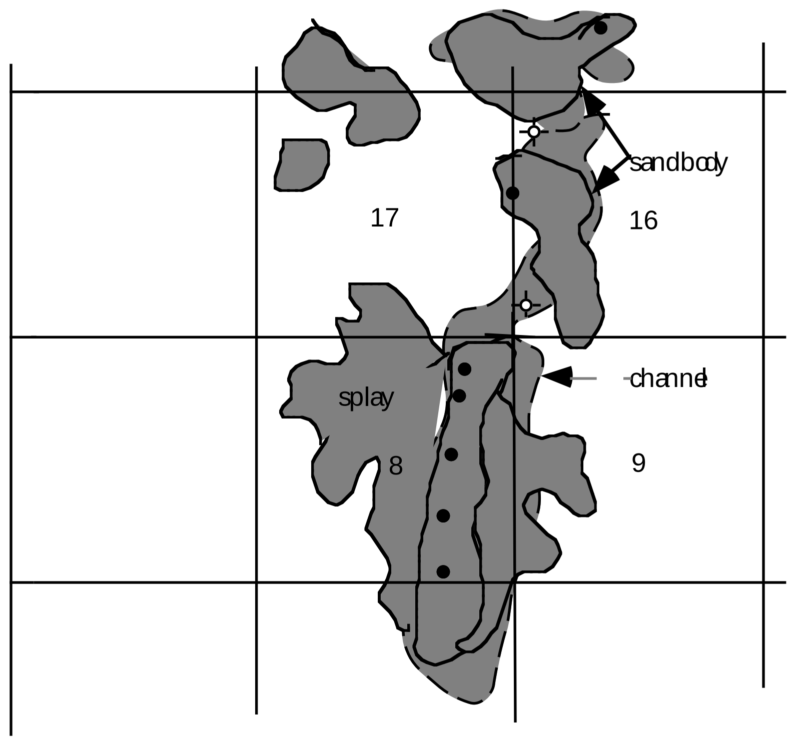

Fig. 20. The interpreted Glauconitic channel sand bodies